Title: Testosterone-Induced Metabolic Changes in Seminal Vesicle Epithelial cells Alter Plasma Components to Enhance Sperm Motility

Authors: Takahiro Yamanaka[1], Zimo Xiao[1], Natsumi Tsujita[1], Mahmoud Awad[1,2], Takashi Umehara[1], Masayuki Shimada[1,3*]

Affiliations:

[1] Graduate School of Integrated Sciences for Life, Hiroshima University; Higashihiroshima, Hiroshima, Japan

[2] Department of Histology, Faculty of Veterinary Medicine, South Valley University; Qena, Egypt

[3] Graduate School of Innovation and Practice for Smart Society, Hiroshima University; Higashihiroshima, Hiroshima, Japan

*Corresponding author. Masayuki Shimada, Ph.D. E-mail: mashimad@hiroshima-u.ac.jp, Tel/Fax: (+81)-824-24-7899

One Sentence Summary: Testosterone induces ACLY expression in seminal vesicles, a key factor in forming seminal plasma to acquire *in vivo* fertilization ability of sperm.

Abstract:

Male factors account for almost half of the causes of infertility. In rodents and humans, most of the components of semen are supplied by the seminal vesicles, and they support male reproductive ability, but there are many unknown details. In this study, the metabolic changes in the seminal vesicle epithelial cells were focused on, and the mechanisms by which testosterone affected the seminal plasma composition were investigated. A factor improving the linear motility of sperm was secreted from the seminal vesicles, and it was produced in an androgen-dependent manner. Bioassays, gene expression, and flux analysis studies demonstrated that testosterone promotes glucose uptake in seminal vesicle epithelial cells via GLUT4, resulting in fatty acid synthesis. ACLY was a critical factor in this metabolic change, which produced fatty acid, especially oleic acid. In conclusion, the critical role of testosterone-induced metabolic changes in the seminal vesicles is to ensure the synthesis of fatty acid. These findings provide new

31 understanding the male fertility mechanisms and may perspective for the development of potential
32 biomarkers of male fertility and advance in the treatment of male infertility.
33

Main Text:

INTRODUCTION

Infertility is defined by the World Health Organization (WHO) as the failure to conceive within 12 months despite contraceptive-free sexual intercourse. Its prevalence has increased over the decades and is observed in 17.5% of couples worldwide *(1)*. The male partner is thought to be solely or in combination responsible for 50% of infertility cases, and the male factor in the etiology of infertility is highly recognized. Male fertility depends largely on the quality of semen composed of sperm and seminal plasma and decreases with aging *(2–4)*.

Sperm that have completed spermatogenesis in the testis acquire their potential to fertilize while maturing in the epididymis *(5–7)*. The physiological change of sperm during fertilization process are collectively referred to as "capacitation". This change includes a large amplitude of flagella (called hyperactivation) and developing the capacity to undergo the acrosome reaction, and can be induced by culturing sperm collected from the epididymis in a medium containing bicarbonate and cholesterol acceptors *(8, 9)*. However, once capacitation is complete, sperm cannot maintain that state for a long time. Therefore, even if epididymal sperm that have not been exposed to seminal plasma are artificially inseminated into the cervix or uterus, the fertilization rate remains low *(10–12)*. That is because, *in vivo*, during ejaculation, exposure of epididymal sperm to seminal plasma masks the unintended capacitation as they pass through the female reproductive tract and ensures fertilization of sperm that reach the oviduct *(13)*. In other words, seminal plasma plays an important role in fine-tuning the timing of sperm capacitation and in maintaining the sustained sperm motility needed to reach the oviduct.

Seminal plasma is mainly produced in the seminal vesicles (approximately 65-75%), with approximately 20-30% produced by the prostate, and small amounts secreted by the bulbourethral and urethral glands *(14)*. The mixing of seminal fluid with accessory reproductive gland fluid during ejaculation causes semen to clot and liquefy in humans and causes vaginal plug formation in rodents. Vaginal plugs not only inhibit continuous mating but also play a role in maintaining sperm in the uterus and ensuring male fertility *(13)*. TGFβ, a component of seminal plasma, increases antigen-specific Treg cells in the uterus of mice and humans, which induces immune tolerance, resulting in pregnancy *(15, 16)*. Furthermore, SVS2, secreted from the seminal vesicle, is also known to be required for sperm to escape attack by the female immune system in the uterus

(17). In addition, seminal plasma contains various biochemical components that support sperm metabolism, including lipids and organic acids. Differences in the relative size of the accessory reproductive glands reflect differences in the seminal plasma composition. Accordingly, there are considerable differences in the properties of seminal plasma between animal species. Specifically, Rosecrans et al. *(18)* found significant differences in the levels of most biochemical components in seminal plasma compared to blood, with specific factors like fructose being rarely detected in blood but abundant in seminal plasma. Our previous studies *(19–21)* documented that seminal plasma also contains creatine and fatty acids taken up by sperm within minutes. These substances play crucial roles in regulating sperm metabolic pathways and enhancing sperm motility. These observations indicate that seminal plasma not only alters the female immune system to protect sperm but also directly influences sperm metabolic pathways, facilitating the transformation of sperm capable of *in vivo* fertilization.

Several specific factors produced by the male accessory glands that contribute to seminal plasma and impact male fertility have been elucidated. For example, surgical removal of seminal vesicles in male mice and rats was associated with infertility *(17, 22, 23)*. The observations that fructose *(24)* and citric acid *(25)* concentrations in seminal plasma of control mice and rats are higher than in castrated animals suggest that the specific metabolism of the accessory glands might be affected by testosterone derived from the testes, which activate intracellular androgen receptors (AR; NR3C4) required for gene regulation of transcription. AR-deficient mice have been found to be infertile *(26)*, and long-term administration of androgen receptor antagonists, like flutamide, abolished male fertility *(27, 28)*. AR-deficient mice and transcriptome analyses have identified specific targets of AR *(29, 30)*. In both mice and humans, androgen levels decrease with aging, and their concentrations have been reported to cause a decrease in male fertility, especially ejaculated sperm motility. In addition to impairments in spermatogenesis, a decline in androgen levels may also disrupt the metabolic functions of the accessory glands and alter the composition of seminal plasma. Therefore, the intricate interplay between testosterone and seminal plasma synthesis in the accessory glands requires further investigation.

In this study, various bioassays were done to identify which accessory glands are essential for sperm fertility. Subsequently, comparative *in vivo* and *in vitro* analyses were performed using a hypoandrogenic model. In addition, biochemical and molecular techniques such as RNA-seq, flux

94 analysis, mass spectrometry, and knockdown experiments were employed. These analyses
95 revealed that testosterone promotes the synthesis of oleic acid in seminal vesicle epithelial cells
96 and its secretion into seminal plasma.
97
98 **RESULTS**
99 **The effect of androgen-dependent changes in mouse seminal vesicle secretions on the**
100 **linear motility of sperm**
101 A direct comparison was conducted to clarify the effects of secretions from the prostate and
102 seminal vesicles on the motility parameters of epididymal sperm. Since it is difficult to collect the
103 ejaculated semen of mice, a pseudo-seminal plasma was prepared using seminal vesicle secretions
104 and homogenized prostate tissue (Fig.1A, Supplemental Fig.1A). When seminal vesicle
105 secretions were added to the HTF medium, the sperm motility, progressive motile, the straight
106 line velocity (VSL), and the percentage of linearity (LIN) values increased significantly compared
107 to when only prostate extract was used. However, the curvi-linear velocity (VCL) did not change
108 (Fig.1B-F). Meanwhile, the secretions from the prostate and seminal vesicles did not affect the
109 viscosity of the medium (Fig.1G). These results indicate that sperm exposure to seminal plasma
110 factors significantly improves sperm linear motility (high VSL and LIN).
111 Androgens regulate the functions of seminal vesicles. Therefore, to elucidate whether the
112 seminal vesicle factors, which enhance sperm linear motility, are synthesized in an androgen-
113 dependent manner, bioassays were performed using seminal vesicle secretions collected from
114 control mice or mice treated daily for 7 consecutive days with flutamide, an androgen receptor
115 antagonist (Fig. 1H, Supplemental Fig.1B). The results showed that Motile, Progressive motile,
116 LIN, and VSL were significantly reduced in the sperm cultured in seminal vesicle secretions from
117 flutamide-treated (Flutamide) compared to the sperm cultured in seminal vesicle secretions from
118 controls (Ctrl) (Fig.1I-L). The reduction of VSL, Motile, and Progressive motile were also
119 significantly lower in the sperm treated with seminal vesicle secretions from over 12 months old
120 mice that showed low circulating testosterone levels as compared with the sperm treated with
121 seminal vesicle secretions from young adult mice (3 months old mice) (Supplemental Fig.2A,B).
122 Furthermore, JC-1 staining to measure mitochondrial membrane potential, which is important for
123 sperm linear motility, showed a significantly lower percentage of high mitochondrial membrane

124 potential in sperm treated with the secretions of seminal vesicles from flutamide-treated mice and
125 over 12 months old mice (Fig.1M, Supplemental Fig.1C,D, Supplemental Fig.2C). Since
126 flutamide treatment and aging also affect spermatogenesis and sperm motility, it should be noted
127 that epididymal sperm donors differ from seminal vesicle donors (Fig. 1H). Due to the strong
128 effect of the decapacitation factor, it was found that seminal vesicle fluid, regardless of the
129 presence or absence of androgens, reduces the fertilization rate in *in vitro* fertilization
130 (Supplemental Figure 1E). The baseline information for the epididymal sperm used in the
131 experiment showed that the sperm were normal (Supplemental Fig.1A). These results indicated
132 that androgen-dependent changes in seminal vesicle functions alter the levels/activity of seminal
133 vesicle secretion factors, which regulate sperm linear motility. The changes in seminal vesicle
134 functions were also induced by aging.
135

136 **Testosterone-androgen receptor activity suppresses the proliferation of seminal vesicle epithelial**
137 **cells**

138 To understand the difference between seminal vesicles that secrete factors for enhancing sperm
139 linear motility and those that are impaired in this function, we performed histological analysis of
140 seminal vesicles recovered from mice treated and non-treated with flutamide. In control mice, the
141 seminal vesicle epithelial cells were in a single layer, and androgen receptors were localized in the
142 nuclei of seminal vesicle epithelial cells (Fig.2A). However, in mice treated with continuous
143 administration of flutamide, seminal vesicle epithelial cells were multilayered, and the strong
144 accumulation of androgen receptors in nucleus was not observed (Fig.2A). To investigate the cause
145 of this multilayering of cells, we performed Ki67 staining, a marker of cell proliferation, and
146 apoptosis detection by TUNEL staining (Fig.2B). The results showed that the percentage of Ki67-
147 positive cells increased significantly after treatment with flutamide, but the percentage of TUNEL-
148 positive cells did not change, suggesting that the testosterone-androgen receptor pathway is
149 responsible for the inhibition of proliferation of seminal vesicle epithelial cells (Fig.2C). These
150 changes of abnormal morphology and high proliferation activity were also observed in seminal
151 vesicle of more than 12 months old mice that showed the low level of testosterone in serum
152 (Supplemental Figure 2D-F). Therefore, seminal vesicle epithelial cells were collected and cultured

153 in primary culture, as shown in Fig. 2D. The changes in cell number were counted, and the cell
154 cycle was analyzed by flow cytometry. When cultured without testosterone (c), the number of
155 seminal vesicle epithelial cells increased time-dependent manner. However, the addition of
156 testosterone significantly decreased the number of seminal vesicle epithelial cells during the 8-day
157 culture period in a concentration-dependent manner (Fig.2E). Flow cytometry on day 7 revealed a
158 significant increase in the proportion of cells in the G0/G1 phase and a corresponding decrease in
159 the G2/M phase. The G2/M phase was significantly decreased by the addition of testosterone (Fig.
160 2F,G). These results indicate that the testosterone-androgen receptor pathway inhibits seminal
161 vesicle epithelial cells in cell division.

162

163 **Testosterone alters metabolic gene expression in seminal vesicle epithelial cells**

164 To better understand the roles of testosterone in suppressing the proliferation of seminal vesicle
165 epithelial cells, RNA sequencing was done using the epithelial cells cultured with or without
166 testosterone. DEG (Differential Expressed Genes) analysis revealed that a total of 23,459 genes
167 were identified, including 997 upregulated genes and 3463 downregulated genes in seminal
168 vesicle epithelial cells by testosterone relative to control (Fig.3A). Genes largely upregulated
169 by testosterone included those already reported in seminal vesicles *(17, 22, 31)*, such as the
170 Seminal Vesicle Secretion (*Svs*) family (*Svs1~6*), *Pate4*, *Spinkl*, *Ceacam10*, and *Sva* (Fig.3B,C).
171 Therefore, the primary culture of seminal vesicle epithelial cells used in this experiment was
172 considered to maintain the characteristics of seminal vesicle epithelial cells *in vivo*. Many genes
173 were downregulated by testosterone, and those with a high rate of variation included collagen
174 synthase and *Mmp2*, which are involved in extracellular matrix formation (Fig.3C). However,
175 KEGG analysis, rather than individual genes, was used to predict functions altered by
176 testosterone. It was found that the expression of genes involved in the metabolic pathway was
177 the most highly affected by testosterone (Fig.3D). Because there is a close relationship between
178 cell proliferation and metabolic activity and between metabolic substrates in seminal plasma and
179 sperm motility, we hypothesized that testosterone induced changes in seminal vesicle epithelial
180 cell metabolism alter the components of seminal plasma to mediate the enhancement of sperm
181 motility.

182

183 **Testosterone shifts the metabolic flux of seminal vesicle epithelial cells**

184 In the presence of testosterone, the addition of glucose significantly activated the extracellular
185 acidification rate (ECAR) normalized by the total number of live cells compared to that in
186 epithelial cells cultured without testosterone (Fig.4A-C). These data indicate that testosterone
187 enhances glucose utilization. This leads to the interpretation that testosterone increases the flow
188 of glycolysis by increasing glucose uptake and alters metabolic flux distribution. To determine
189 the metabolic fate of glycolytic end products, seminal vesicle epithelial cells were cultured with
190 and without testosterone. Subsequently, the concentrations of pyruvate and lactate in the culture
191 supernatant normalized by the total number of live cells were measured. The addition of
192 testosterone significantly decreased the pyruvate concentration; however, the lactate
193 concentration did not change significantly (Fig.4D,E). Therefore, we analyzed mitochondrial
194 metabolism using a flux analyzer, predicting that more glucose is metabolized, pyruvate is metabolized
195 from phosphoenolpyruvic acid through glycolysis in response to testosterone, and is further
196 metabolized in the mitochondria. Unexpectedly, when measuring mitochondrial respiratory
197 metabolism normalized by the total number of live cells with a Flux analyzer, the basal respiratory
198 rate (the electron transport chain activity) was significantly decreased by testosterone (Fig.4F-
199 J). Oligomycin-sensitive respiration was also significantly suppressed by exposure to testosterone.
200 Furthermore, the FCCP uncoupled respiration and spare respiration capacity were also
201 significantly decreased in response to testosterone treatment. Overall, these data indicate that
202 testosterone promotes the redistribution of metabolic flux. In other words, testosterone increased
203 glycolysis in seminal vesicle epithelial cells while decreasing mitochondrial respiration. To
204 determine whether these changes were accompanied by changes in gene expression of specific
205 metabolic-related enzymes, we analyzed gene expression levels.

206

207 **Testosterone causes changes in the expression of genes encoding enzymes involved in glucose**
208 **catabolism and anabolism**

209 The expression of genes involved in glucose catabolism and anabolism in the *in vitro* culture
210 system of seminal vesicle epithelial cells was analyzed by qPCR (Fig.5). The gene expression of
211 glucose transporter (*Glut*) and enzymes involved in the glycolytic pathway was not significantly

212 affected by testosterone, consistent with the results of metabolic flux analysis, which showed that
213 the glycolytic pathway was not enhanced despite the activation of the glycolysis. Furthermore,
214 testosterone did not significantly affect the expression of genes encoding enzymes involved in the
215 TCA cycle in mitochondria. However, the expression of enzymes involved in the electron
216 transport chain was significantly decreased. Interestingly, testosterone significantly increased the
217 expression of Acly, which encodes a cytoplasmic enzyme that converts citrate transported from
218 the TCA cycle into acetyl-CoA, a substrate that is essential for fatty acid synthesis. Although
219 *Hmgcr*, which encodes the rate-limiting enzyme involved in cholesterol synthesis, was unchanged,
220 the expression of *Acc*, which encodes the rate-limiting enzyme for fatty acid synthesis, was
221 significantly upregulated by testosterone. These characteristic testosterone-induced changes in
222 gene expression observed in cultured cells were also detected by ACLY immunostaining of *in*
223 *vivo* seminal vesicle samples (Supplemental Figure 3). Specifically, the expression of genes
224 encoding a group of enzymes of the electron transport chain (*mtNd6*) was significantly
225 upregulated by continuous flutamide administration *in vivo*, whereas the gene expression of *Acly*
226 and *Acc* was significantly decreased by flutamide administration (Supplemental Figure 3B).
227 Immunostaining results showed that ACLY was detected specifically in seminal vesicle epithelial
228 cells, and their staining appeared to be reduced by flutamide treatment. The lower level of ACLY
229 was also observed in seminal vesicle epithelial cells of over 12 months old mice (Supplemental
230 Figure 3C).
231
232 **Mechanism of testosterone-induced enhancement of glucose uptake and, thereby, fatty acid**
233 **synthesis**
234 Since it is known that testosterone regulates the intracellular localization of GLUT4, we
235 focused on the intracellular localization of GLUT4 and its glucose uptake capacity *(32, 33)*.
236 The effect of testosterone on glucose uptake in seminal vesicle epithelial cells was analyzed
237 using fluorescence-labeled glucose. As expected from the results of flux metabolic analyses,
238 testosterone treatment significantly increased glucose uptake (Fig.6A). Indinavir, a functional
239 inhibitor of GLUT4, significantly suppressed glucose uptake and significantly decreased fatty
240 acid synthesis (the amount of fatty acids accumulated in the cell), which was increased by
241 testosterone (Fig.6A,B).

242 Furthermore, immunostaining analysis of the localization of GLUT4 in seminal vesicles
243 revealed that GLUT4 was translocated outside the nucleus of seminal vesicle epithelial cells
244 under the presence of testosterone (Fig.6C). These data suggest that GLUT4 was partially
245 localized at the plasma membrane and contributed to glucose uptake. In contrast, in seminal
246 vesicles from mice treated with flutamide continuously, no strong signal was detected at the
247 presumed location of GLUT4 near the plasma membrane of seminal vesicle epithelial cells, even
248 though the protein expression level was not affected (Fig.6C,D). The same characteristics were
249 observed in aged mice.
250 Qualitative and quantitative analysis of the fatty acids synthesis was performed by GC-MS.
251 In seminal vesicles, C16:0, C18:0, and C18:1 were detected, in which C18:1 was decreased to
252 an undetectable level in seminal vesicles of mice treated with the flutamide (Supplemental
253 Figure 4A). In the cultured seminal vesicle epithelial cells, C18:1, oleic acid, was significantly
254 increased by the addition of testosterone as observed in the seminal vesicle (Fig.6E). The
255 expression of *Elovl6* encoding ELOVL6, which desaturates C18:0 saturated fatty acids to C18:1,
256 was significantly up-regulated by testosterone (Fig.6F,G). The testosterone-induced change was
257 also detected in *in vivo* samples (seminal vesicle), where the expression of *Elovl6* was decreased
258 by the flutamide treatment (Supplemental Figure 4B).
259 In order to examine whether these lipids are the factors that induces sperm linear motility, we
260 examined whether or not the addition of lipid mixture changed in sperm motility pattern
261 (Supplemental Figure 5). The lipid mixture did not affect sperm motility at any concentration
262 compared to the control (LM 0%). However, VSL was significantly increased in sperm with 1%
263 lipid mixture added.
264
265 **ACLY expression is upregulated by testosterone and is essential for the metabolic shift of**
266 **seminal vesicle epithelial cells that mediates sperm linear motility**
267 ACLY is upregulated in seminal vesicle epithelial cells as a factor that enables the utilization
268 of citric acid from the TCA cycle for fatty acid synthesis outside the mitochondria. Therefore,
269 we performed siRNA knockdown experiments on ACLY to clarify the impact of ACLY on the
270 cellular metabolic shift. The addition of testosterone significantly increased the amount of ACLY
271 protein in seminal vesicle epithelial cells (Fig.7A,B). Viral infection with siRNAs encoding *Acly-*

272 targeted siRNAs markedly decreased the amount of ACLY (Fig.7C). When ACLY was knocked
273 down using shRNA, the proliferation arrest caused by testosterone was released, and the cells
274 began to proliferate again (Fig.7D). This knockdown of ACLY increased the oxygen
275 consumption of seminal vesicle epithelial cells in the control and testosterone-treated group
276 (Fig.7E,F). Thus, ACLY expression is associated with mitochondrial metabolic pathway activity
277 in seminal vesicle epithelial cells. Furthermore, the knockdown of ACLY also significantly
278 suppressed testosterone-induced fatty acid synthesis in seminal vesicle epithelial cells (Fig.7G).
279 According to the GC-MS quantification results, the amount of fatty acids secreted into the
280 culture medium was also reduced by ACLY knockdown. In particular, the enhancement of oleic
281 acid secretion by testosterone was inhibited by ACLY knockdown (Fig.7H-J). Supernatants from
282 epithelial cells of the testosterone-added group induced motility and linear motility (Highest
283 VSL and LIN; Fig.7K-N). However, the knockdown of ACLY significantly reduced the effects
284 of the culture supernatant on sperm motility and LIN (Fig.7K-N). These results found that cell
285 proliferation stops when a metabolic shift mediated by ACLY occurs, and glucose is reallocated
286 to fatty acid synthesis. Fatty acid synthesis is an important function of the seminal vesicles, and
287 it was found that when testosterone is present, fatty acid synthesis enhancement and cell
288 proliferation stop simultaneously. However, it is not known what effects occur when cell
289 proliferation stops.
290
291 **This characteristic metabolic mechanism induced by testosterone is also observed in**
292 **human seminal vesicle epithelial cells**
293 To determine whether these findings in mice could be applied to humans, the commercially
294 available human seminal vesicle epithelial cells were used for following studies (Fig.8A). The
295 growth curves showed that cell proliferation was inhibited by 100 ng/mL of testosterone
296 compared to the control; a pattern similar to that observed in murine seminal vesicle epithelial
297 cells (Fig.8B). The characteristics of metabolic activity of human seminal vesicle epithelial cells
298 were also similar to those of mice, with testosterone significantly enhancing the ECAR response
299 (Fig.8C-E), but significantly reducing the capacity for oxygen consumption in mitochondria
300 (Fig.8F-H). Moreover, fluorescent-glucose uptake was increased by testosterone and decreased
301 by the inhibitor of GLUT4 function (Fig.8I). Additionally, while testosterone also significantly

302 increased fatty acid synthesis, this increase was completely abolished by the GLUT4 inhibitor
303 (Fig.8J). According to the quantitative results obtained using GC-MS, the amount of fatty acids
304 secreted into the culture medium also decreased due to the inhibition of GLUT4 by indinavir. In
305 particular, it was shown that oleic acid secretion is completely dependent on glucose via GLUT4
306 (Fig.8K-M).
307
308 **DISCUSSION**
309 Seminal plasma has a variety of functions, including sperm transport, nutritional support,
310 interactions with the female reproductive tract, and especially the regulation of its relationship
311 with the female immune system. Mammalian seminal plasma is secreted mainly from the
312 seminal vesicle and is rich in cytokines, prostaglandins, and SVS family members *(34)*. For this
313 reason, recent studies have focused on the immunomodulatory function of seminal plasma in the
314 female reproductive tract. On the other hand, fructose and lipids in seminal plasma are the major
315 energy sources for sperm *(35)*. However, although metabolomic analyses of seminal plasma
316 have shown that metabolic substrates are present at higher concentrations in seminal plasma than
317 in blood *(18, 24, 25)*, how these substrates are synthesized and specifically how they alter sperm
318 motility has not been determined. Moreover, though the motility of ejaculated spermatozoa is
319 known to decrease with aging, few reports have revealed age-related changes in the seminal
320 vesicles, which are responsible for seminal plasma synthesis.
321 In this study, we focused on the reproductive organs that synthesize seminal vesicle secretion
322 as target organs for testosterone and found that factors formed by testosterone-dependent
323 metabolic changes in seminal vesicles activate sperm mitochondria and enhance their linear
324 motility. Testosterone is known to activate intracellular ARs and alter intracellular metabolic
325 pathways in skeletal muscle *(36)*, prostate cells *(37)* and cardiomyocytes *(33)*. ARs are known
326 to directly regulate the expression of glycolytic and lipid metabolic genes *(33, 38, 39)*. In the
327 present study, the nuclear localization of AR in seminal vesicle epithelial cells (i.e., functioning
328 as a transcription factor) and the activation of the glycolytic system by testosterone were similar
329 to those in the above cell types. In seminal vesicle epithelial cells, an increased trend in the
330 expression of *Glut3* and an enhancement of GLUT4 function were observed in a testosterone-
331 dependent manner. Such effects of testosterone on glucose metabolism have also been reported

332 in skeletal muscle, liver, and adipose tissue, where testosterone leads to the phosphorylation of
333 GLUT4 and enhances its translocation to the plasma membrane *(40, 41)*. This is consistent with
334 the results of our metabolic flux analyses, which show that testosterone increases the rate of
335 glycolysis in seminal vesicle epithelial cells by increasing glucose uptake. We further confirmed
336 that GLUT4 is the transporter that mediates this glucose uptake using indinavir, a GLUT4-
337 specific inhibitor.

338 This study suggests that fatty acid synthesis is an important function of the seminal vesicles,
339 which provide an environment where the ejaculated sperm can carry out active metabolism. The
340 shift to fatty acid synthesis was consistent with the cessation of cell proliferation in the presence
341 of testosterone. This mechanism could prevent the seminal vesicles from excessively consuming
342 the substrates necessary for sperm motility. Manipulation of ACLY expression in mouse
343 myoblasts and embryonic stem cells has been shown to alter the TCA cycle into a "non-normal
344 cycle" *(42)*. One advantage of the non-normal TCA cycle is its ability to retain carbon instead
345 of combusting it and to regenerate the cytosolic NAD+ needed to maintain glycolysis *(42, 43)*.
346 It suggests that ACLY, activated by testosterone, may suppress proliferation by skipping several
347 steps in the mitochondrial TCA cycle and minimizing ATP production associated with aerobic
348 respiration in seminal vesicle epithelial cells.

349 Testosterone has been reported to cause hypertrophy of cardiac myocytes *(44, 45)*. Cell
350 hypertrophy is partly due to the accumulation of fatty acids in the cytoplasm, which causes
351 significant damage to cellular functions *(46, 47)*. On the other hand, normal cell hypertrophy,
352 especially in myofibers, involves the activation of signaling molecules such as Myc, hypoxia-
353 inducible factor, and Pi3k-Akt-mTor, which regulate metabolic reprogramming in cancer by
354 increasing glucose uptake in the presence of oxygen *(48–50)*. In the present study, induction of
355 ACLY expression by testosterone not only decreased cycling in the TCA cycle, but also promoted
356 glucose assimilation, which played an important role in fatty acid synthesis. Thus, in tissues
357 where fatty acid synthesis is promoted, either β-oxidation-dependent ATP production in
358 mitochondria or the secretion of fatty acids occurs to maintain cellular function *(51–53)*
359 providing evidence to explain why the presence of fatty acids in the cell has no adverse effect.
360 In accessory reproductive glands, such as the prostate and seminal vesicles, the glucose uptake
361 is activated in a testosterone dependent. However, mitochondrial respiration is not enhanced,

362 cell proliferation is not induced, and the metabolites are used as a substrate for sperm motility.
363 This may be because, in the prostate, pyruvate synthesized by the glycolytic system in response
364 to testosterone is converted to acetyl CoA, which is then converted to citric acid in the TCA
365 cycle, citric acid is released as the main component of seminal plasma *(37)*.

366 The testosterone-dependent growth of cancerous prostate epithelial cells may be due to genetic
367 mutations, such as elevated expression of the gene encoding aconitase, which converts citric acid
368 to isocitrate, which blocks the TCA cycle and inhibits citric acid secretion *(54)*. On the other
369 hand, in the analysis of seminal vesicle epithelial cells, testosterone treatment induced the
370 expression of *Acc*, which encodes the rate-limiting enzyme for fatty acid synthesis, and *Elovl6*,
371 which desaturates to oleic acid, significantly increasing total saturated fatty acid and oleic acid
372 content. Therefore, testosterone promotes glucose conversion into fatty acids, especially oleic
373 acid, in seminal vesicle epithelial cells. Although there is a commonality in the activation of the
374 glycolytic system testosterone target tissues, the different expression patterns of genes involved
375 in metabolism in mitochondria may exert their specific functions in each tissue. In addition to
376 genes involved in fatty acid synthesis such as *Fasn* and *Elovl6*, *Acly* is also encoded in a region
377 in close proximity to human chromosome 17 and mouse chromosome 11, suggesting that in
378 seminal vesicle epithelial cells, this region is targeted to promote gene expression. The co-
379 regulation of these genes in seminal vesicle epithelial cells leads to synthesizing the fatty acids.

380 Decreased testosterone synthesis in the testes is a phenomenon observed with aging associated
381 with decreased spermatogenesis *(55)*. However, the probability of obtaining sperm without ICSI
382 or IVF is extremely low, despite the presence of sufficient numbers of sperm with normal-
383 morphology *(56–58)*. This indicates that testosterone plays a major role not only in
384 spermatogenesis but also in the functional maturation of sperm. In this study, metabolic
385 abnormalities induced by inhibition of androgen receptor function caused abnormal proliferation
386 of seminal vesicle epithelial cells in aged mice. In other words, the findings of the seminal vesicle
387 epithelial cell culture experiments and flutamide treatment may mimic the changes that occur
388 with aging. Oleic acid synthesis by testosterone-dependent metabolic pathways was regulated in
389 seminal vesicle epithelial cells. It could be assumed that a decrease in testosterone levels causes
390 abnormalities in the components of human semen. In particular, the results open up the

391 possibility of a translational study to detect low testosterone levels in men by testing for oleic
392 acid in semen.
393 Because seminal plasma contains components specific to certain male reproductive organs,
394 differences in protein composition may reflect pathological processes in these specific organs
395 *(59)*. However, although proteomic and metabolomic analyses of seminal plasma have been
396 performed *(31, 59)*, the functional changes in seminal plasma, especially the effects on *in vivo*
397 fertilization potential, are not fully understood. This is because there are many challenges to
398 measuring the direct relationship between sperm metabolism and movement patterns. It has been
399 suggested that the potential importance of the effect of oleic acid on improving fertility, yet it is
400 too early to conclude this in this study. If a direct causal relationship between fatty acid
401 composition and improved sperm motility is established, differences in the concentration of fatty
402 acids in the seminal plasma will become a predictive marker of the fertilizing ability of semen.
403 The interspecies differences between humans and mice should be interpreted with caution, and
404 the translational aspects to humans are speculative, but this study revealed a testosterone-
405 dependent mechanism of oleic acid production in seminal vesicle epithelium.
406 Overall, the results of the studies described herein strongly support the hypothesis that
407 testosterone-dependent glucose to oleic acid conversion processes are required for normal
408 seminal plasma functions in the seminal vesicle (Fig.9). This study advances our understanding
409 of the role of testosterone in glucose metabolism and fatty acid synthesis and lays the
410 groundwork for future research in reproductive biology and fertility.
411
412 **MATERIALS AND METHODS**
413 **Study design**
414 The objective of this study was to elucidate the mechanisms of seminal plasma synthesis.
415 Testosterone-dependent changes in the seminal plasma function were examined by comparative
416 analysis of adult mice and flutamide-treated mice. The bioassays of extracts from male accessory
417 glands by epididymal sperm motility analysis were used to examine the seminal plasma
418 components important for sperm function. We also isolated the mouse seminal vesicle epithelial
419 cultured cells, and investigated the synthesis mechanism of the seminal plasma components using

420 RNA-seq, FluxAnalyzer, and shRNA knockdown. Finally, we performed validation using the
421 human epithelial cells.
422
423 **Chemicals and Animals**
424 Unless otherwise noted, chemicals used in this study were purchased from Sigma-Aldrich (St.
425 Louis, MO, USA) or Nacalai tesque (Osaka, Japan). Pregnant mare serum gonadotropin (PMSG)
426 and human chorionic gonadotropin (hCG) were purchased from Asuka Seiyaku (Tokyo, Japan).
427 All procedures during animal experiments were reviewed and approved by the Animal Care and
428 Use Committee of Hiroshima University (Hiroshima, Japan; C21-9-3) and conducted according
429 to regulations. Specific pathogen-free C57BL/6NCrl male mice or Crl: CD1 (ICR) female mice
430 were purchased from Jackson Laboratory Japan (Kanagawa, Japan) and housed in an
431 environmentally controlled room with a 12-hour light/dark cycle, a temperature of 23 ± 3°C, and
432 free access to laboratory food (MF; Oriental Yeast Co., Ltd., Tokyo, Japan) and tap water. 8- to
433 16-week-old male or female mice were used for the experiments. Flutamide-treated mice were
434 injected subcutaneously for 7 days with 50 μg/g (body weight) of flutamide dissolved in corn oil.
435 Vehicle-treated mice received 100 μL of corn oil subcutaneously for 7 days. The aged males were
436 12 to 16 months old.
437
438 **Bioassay using pseudo-seminal plasma and epididymal sperm**
439 Prostate (mixed anterior, dorsal, lateral, and ventral) and seminal vesicles were collected from
440 adult C57BL/6NCrl mice. Seminal vesicle secretions were obtained by pressing the seminal
441 vesicles immediately after euthanasia. Prostatic extracts were obtained by homogenizing the
442 prostate immediately after euthanasia. Seminal vesicle secretions and prostate extracts collected
443 from one male mouse were dissolved in 500 μL and 200 μL of mHTF medium without BSA *(60)*,
444 respectively, then centrifuged at 2000 × g for 5 min at room temperature, and the supernatant was
445 collected, and protein levels were determined. The seminal vesicle secretions from flutamide-
446 treated mice were also collected similarly.
447 Cauda epididymis sperm recovered from male mouse were dispersed in 500 μL of mHTF
448 without BSA and centrifuged at 300 × g, 3 min to wash out epididymis-derived factors. The final
449 protein concentration of prostate and seminal vesicle secretion was adjusted to 10 mg/mL. An

450 aliquot (2 mL) of the pooled prostate or seminal vesicle extracts was conducted the viscosity
451 measurement data using Tuning Fork Vibro Viscometers (SV-1A, A&D Company, Tokyo, Japan).
452 The epididymis sperm was mixed with seminal vesicle secretion and/or prostate extract as shown
453 in Fig.1 and Supplementary Figure 1. The samples were incubated at 37°C for 60 min in a
454 humidified atmosphere of 5% CO2 in air. Sperm motility patterns were then examined using
455 computer-assisted sperm analysis (CASA; HT CASA-Ceros II, Hamilton Thorne, Beverly, MA,
456 USA), with software version 1.11.9. The following sperm motility parameters were analyzed:
457 percentage of motile sperm (denoted by a path velocity >40 μm/s and a VSL >20%), percentage
458 of motile sperm with progressive motility (denoted by a path velocity >40 μm/s and a straightness
459 ratio >60%). Straight-Line Velocity; VSL: The distance between the first and last tracking points
460 of the sperm trajectory divided by the elapsed time. Curvi-Linear Velocity; VCL: The sum of the
461 distances between the centers of brightness in each frame divided by the elapsed time. Linearity;
462 LIN: Measures the straightness of the path. LIN is derived from the ratio of VSL/VCL multiplied
463 by 100.
464
465 **Serum testosterone levels**
466 The serum was separated from the clot by centrifugation at 1,500 × g for 15 min. Testosterone
467 levels in the serum samples were determined by a rodent testosterone ELISA test kit (ERKR7016,
468 Endocrine Technologies, Inc., Newark, CA, USA) according to the manufacturer's manual.
469
470 **Mitochondrial activity**
471 Mitochondrial activity of sperm was measured using a MitoPT® JC-1 Assay Kit (911, Immuno
472 Chemistry Technologies, LLC, Bloomington, MN, USA) according to our previous study *(20)*.
473 Briefly, sperm were incubated with 200 μL of working solution containing 5,5',6,6'-tetrachloro-
474 1,1',3,3'-tetraethylbenzimidazolyl carbocyanine iodide (JC-1) dye at 37 °C for 30 min in the dark.
475 Using 10 μM of antimycin control (A8674; Sigma) under the same incubation conditions, we
476 confirmed that the JC-1 reaction is sensitive to changes in membrane potential. The sperm
477 suspension was centrifuged and washed twice with the base medium. After washing, the sperm
478 pellet was resuspended in the base medium and analyzed with an Attune® NxT Acoustic Focusing
479 Cytometer (Thermo Fisher Scientific Inc., Waltham, MA, USA) using a 488 nm laser and a filter

480 with a bandwidth of 574/26 nm. The intensity of the average value was analyzed as the mean
481 fluorescence intensity (MFI) of JC-1 orange aggregates. A total of 100,000 sperm events were
482 analyzed. The sperm population is shown in Supplementary Figure 6.
483
484 ***In vitro* fertilization (IVF)**
485 3 weeks old CD1 female mice were injected intraperitoneally with 4IU eCG to stimulate
486 follicle development and 5 IU hCG at 48 hours later. COCs collected from the oviductal
487 ampulla 16 h after hCG injection were placed into 100 μL of human tubal fluid (HTF) medium.
488 Sperm were collected from the cauda epididymis of 15 weeks or older C57BL/6N male mice in
489 100 μL of HTF medium. After 60 min of incubation with or without treatments (Ctrl, Flu or
490 HTF), the sperm were added into HTF medium at a final concentration of
491 2×10^5 spermatozoa/mL, and coincubated with the COCs. After 6h incubation, oocytes were
492 washed three times thoroughly and cultured in 250 μL of KSOM medium (MR 106-D; Sigma).
493 The cleavage rate was determined on Day 1 (Day 0=day of IVF), and the appearance of
494 blastocysts was recorded on Day 5.
495
496 **Immunohistochemistry and immunofluorescence**
497 Seminal vesicles were fixed overnight in 4% (w/v) paraformaldehyde/PBS, dehydrated in 70%
498 (v/v) ethanol, and embedded in paraffin. Paraffin-embedded fixed sections (4 μm) were
499 deparaffinized and hydrated with xylene and ethanol, respectively. Some slides were stained with
500 hematoxylin and eosin (HE). For antigen retrieval, sections were placed in citrate buffer (pH 6.0),
501 microwaved until boiling and allowed to stand at the temperature of pre-boil (95°C) for 15
502 minutes. Sections were incubated with 3% (v/v) hydrogen peroxide in methanol to block
503 endogenous peroxidase and then incubated with Normal Goat Serum Blocking Solution for rabbit
504 antibody (S-1000, Vector Laboratories, Newark, CA, USA) to block nonspecific sites. The
505 sections were then incubated overnight with primary rabbit antibodies: anti-AR antibody (1:100;
506 ab133273; Abcam, Cambridge, UK), anti-Ki67 antibody (1:1000; ab15580; Abcam) or anti-
507 ACLY antibody (1:200; ab40793; Abcam). Positive signals were visualized by DAB (3,3′-
508 Diaminobenzidine, 040-27001, Fujifilm Wako, Osaka, Japan) using the VECTASTAINE
509 LifeABC kit (PK-6101, Vector Laboratories) according to the manufacturer's protocol. Apoptotic

510 cells (including fragmented DNA) were detected using the In Situ Cell Death Detection Kit POD
511 (11684817910, Roche Ltd., Basel, Switzerland). To avoid false-positive or false-negative results,
512 DNAse-treated sections were used as positive controls, and TdT-untreated sections were used as
513 negative controls for apoptosis.
514 Nuclei were visualized with hematoxylin (Sakura Finetek, Tokyo, Japan). Ki-67 and apoptotic
515 positive cells were quantified using ImageJ software (National Institutes of Health; Bethesda, MD,
516 USA), with software version 2.1.0/1.53u. Randomly selected sections were stained, and images
517 were obtained from randomly selected fields in each section. The positive percentage is defined
518 as the percentage of positively stained cells in the total number of epithelial cells evaluated. Only
519 positive staining was considered, regardless of staining intensity. For immunofluorescence, after
520 blocking nonspecific sites, the sections were incubated with a primary antibody: anti-GLUT4
521 antibody (1:200; ab33780; Abcam). After washing with 0.3% (v/v) Triton X-100 in PBS (-), Cy3-
522 labeled goat anti-rabbit IgG (1:200, C-2306, Sigma) and DAPI (VECTESHIELD Mounting
523 Medium with DAPI, H-1200, Vector Laboratories) were used to visualize the antigen and nuclei.
524 Digital images were taken using an APX100 Digital Imaging System and CellSens imaging
525 software (EVIDENT, Tokyo, Japan), with software version 4.1.1.
526
527 **Isolation and culture of seminal vesicle epithelial cells**
528 Seminal vesicles were removed from euthanized mice, cut open vertically to expose the seminal
529 vesicle cavity, and incubated with Hanks' balanced salt solution (HBSS; $CaCl_2 \cdot 2H_2O$ 0.185 g/L,
530 $MgSO_4$ 0.098 g/L, KCl 0.400 g/L, KH_2PO_4 0.060 g/L, NaHCO3 0.350 g/L, NaCl 8.000 g/L,
531 Na_2HPO_4 0.048 g/L, D-Glucose 1.0 g/L, dissolved in ultrapure water). Tissues were digested with
532 10 mL of HBSS containing 25 mg/mL pancreatin and 0.25% (v/v) trypsin EDTA for 1 hour at
533 4°C, 45 minutes at room temperature, and 15 minutes at 37°C, and epithelial cells were obtained.
534 These were passed through a 70 μm nylon filter (352350, Corning Inc., Corning, NY, USA) and
535 seeded into collagen-coated 12-well plates (4815-010, IWAKI, Shizuoka, Japan). Cells were
536 cultured in DMEM/F-12, 10% fetal bovine serum (FBS; 10438-018, Thermo Fisher Scientific
537 Inc.), 100 U/mL penicillin, 100 μg/mL streptomycin. The culture condition was 37°C, 5% CO_2,
538 95% air, and humidity.

539 Human seminal vesicle epithelial cells (4460, ScienCell Research Laboratories, Carlsbad, CA,
540 USA) were purchased, seeded in 2 μg/cm^2 poly-L-lysine-coated plates, and cultured in epithelial
541 cell medium (4101, ScienCell Research Laboratories). The cells were seeded at 10000 cells/cm^2
542 on collagen-coated plates the day before 100 ng/mL testosterone treatment. Testosterone was
543 dissolved in ethanol, and the final concentration of ethanol was adjusted to 0.1% (v/v) when used
544 for cultured cells. The culture medium was replaced every 48 hours.
545
546 **Cell proliferation curve**
547 The seminal vesicle epithelial cells were seeded at 10000 cells/cm^2 and then were cultured in
548 various concentrations of testosterone. The cells were washed with HBSS (without $CaCl_2$-
549 $2H_2O/MgSO_4$) at the time of cell counting and collected using 0.25% (v/v) trypsin. The recovered
550 cells were suspended in DMEM/F-12 medium, and cell numbers were determined using an
551 Automated Cell Counter TC20TM (BIO-RAD Laboratories, Hercules, CA, USA) to calculate the
552 number of cells contained per well (4 cm^2).
553
554 **Cell cycle analysis**
555 The recovered cells as described above were fixed in 2-5 ml of cold (4°C) 70% methanol for
556 at least 30 minutes on ice. After centrifugation at 500g for 5 minutes at 4°C to obtain pellets, the
557 cell pellet was suspended in 50 μM propidium iodide and 20 × diluted RNase (19101, QIAGEN
558 Inc., Venlo, Netherlands) and then were incubated at 37°C for 30 minutes. After twice washing
559 with 1 ml of PBS at 300 g for 3 min at 4°C, the cells were analyzed by flow cytometry. The cell
560 population is shown in Supplementary Figure 8. A total of 20,000 events were analyzed.
561
562 **RNA-sequencing**
563 Total RNA was extracted from cells using the RNeasy Mini Kit (74106, QIAGEN). Three
564 independent samples were assayed to evaluate the reproducibility of the experimental procedures.
565 The quality of total RNA (1 μg) submitted for sequencing was checked using a Bioanalyzer
566 (Agilent Technologies Inc., Santa Clara, CA, USA), and all RNA integrity numbers were >7.0.
567 The libraries for RNA sequencing were sequenced with 2 × 150-bp paired-end reads on a
568 NovaSeq6000 (Illumina Inc., San Diego, CA, USA). The obtained sequencing data were analyzed

569 using RaNA-seq *(61)*, an open bioinformatics tool for rapid RNA-seq data analysis. FASTQ files
570 were preprocessed in the pipeline using the Fastp tool, and expression was quantified using
571 Salmon. DEseq2 was used to identify differentially expressed genes (DEGs) with adjusted p-
572 values less than 0.05 between the testosterone-treated groups in transcripts per million (TPM)
573 between control and testosterone-treated cells. The pathways were identified from the KEGG
574 database on RaNA-seq.
575
576 **Extracellular flux analysis**
577 Oxygen consumption rate (OCR) and ECAR were measured using an extracellular flux
578 analyzer (XF HS Mini; Agilent Technologies). Eight-well plates for the XF HS Mini were coated
579 with fibronectin (5 μg/mL, F1141, Sigma-Aldrich) dissolved in phosphate-buffered saline (PBS),
580 incubated overnight, and then washed with Roswell Park Memorial Laboratory medium for XF
581 (Roswell Park Memorial Institute medium; RPMI, 103576-100, Agilent Technologies; containing
582 1% FBS) for XF before analysis. Mouse seminal vesicle epithelial cells or human seminal vesicle
583 epithelial cells treated with 100 ng/mL testosterone for 7 days were suspended in RPMI medium
584 at a concentration of 10,000 cells/180 μL, or mouse seminal vesicle epithelial cells infected with
585 shRNA were suspended at a concentration of 2000 cells/180 μL in each well. After centrifugation
586 at 300 × g for 3 minutes, the plates were placed in an incubator at 37°C and 100% air and used
587 for analysis within 1 hour.
588 For glucose metabolism assessment, cells were sequentially treated as indicated with D-
589 Glucose (10 mM; 103577-100, Agilent Technologies), Oligomycin (1 μM; O4876, Sigma-
590 Aldrich), and 2-Deoxy-Glucose (50 mM; D8375, Sigma-Aldrich).
591 For mitochondrial respiration measurement, cells were sequentially treated as indicated with
592 Oligomycin (1 μM), carbonyl cyanide 4-(trifluoromethoxy) phenylhydrazone (FCCP; 5 μM,
593 SML2959, Sigma-Aldrich), and Rotenone (1 μM; R8875, Sigma-Aldrich)/Antimycin A (1 μM;
594 A8674, Sigma-Aldrich). Cellular metabolism readouts, such as glycolysis, glycolytic reserve,
595 basal OCR, Maximum respiration, ATP Production, Spare respiratory capacity, were determined
596 using the Agilent Seahorse Wave software with software version 3.0.0.41. However, to avoid
597 many ambiguities and problems with interpretation, “glycolysis” is written as “Glucose-induced

598 ECAR", "glycolytic reserve" as "Oligomycin-sensitive ECAR", "maximum respiration" as
599 "FCCP uncoupled respiration", and "ATP production" as "Oligomycin-sensitive respiration".
600
601 **Measurement of pyruvate and lactic acid**
602 For measurements, mouse or human seminal vesicle epithelial cells were treated with 100
603 ng/ml testosterone for 6 days. The culture supernatant was collected after 24 hr of additional
604 culture. Pyruvate consumption was measured using the Pyruvate Assay kit (MET-5029, Cell
605 Biolabs, Inc., San Diego, CA, USA). The fluorescence intensity was measured using a microplate
606 reader (ex. 570 nm/em. 615 nm). Lactate released into the medium was measured using the
607 Lactate Assay kit (L256, DOJINDO LABOLATORIES Co., Ltd., Kumamoto, Japan). The
608 absorbance was measured using a microplate reader (wave length=450nm).
609
610 **qPCR**
611 The cDNA was synthesized from 40 ng of total RNA using oligo$(dT)_{15}$ primers (3805, Takara
612 Bio Inc., Shiga, Japan) and an Avian myeloblastosis virus (AMV) reverse transcriptase from
613 Promega (M5101, Madison, WI, USA). The cDNA and primers were added to Power SYBR
614 Green PCR Master Mix (4367659, Applied Biosystems, Foster City, CA, USA) in a total reaction
615 volume of 15 µl. Conditions were set to the following parameters: 10 min at 95°C, 15 sec at 95°C,
616 and 1 min at 60°C. Cycles were repeated 45 times. Specific primer pairs were selected and
617 analyzed, as shown in Table S1. Expression was first normalized to housekeeping gene *Rpl19*,
618 and fold change was calculated relative to the mean of the control samples.
619
620 **Glucose uptake test of seminal vesicle epithelial cells and lipid determination of culture**
621 **supernatants**
622 Mouse or human seminal vesicle epithelial cells treated with or without 100 ng/mL testosterone
623 for 6 days were used for this experiment. Cells were treated with or without the GLUT4 inhibitor
624 indinavir (100 nM) and 100 ng/mL testosterone for an additional 24 hours. Collected 15,000 cells
625 were subjected to Glucose Uptake Assay Kit-Green (UP02; DOJINDO), and fluorescence
626 intensity was measured using a microplate reader (ex. 485 nm/em. 535 nm).

627 Total lipid content in cultured medium was quantified using a lipid quantification kit (STA-617
628 Fluorometric, Cell Biolabs, Inc.) according to the manufacturer's protocol. The fluorescence
629 intensity was measured using a microplate reader (ex. 485 nm/em. 535 nm).
630
631 **Gas chromatography-mass spectrometry analysis**
632 Fatty acid measurements in culture supernatant and seminal vesicle secretions were done
633 according to our previous work *(21)*. Fatty acids in the samples were extracted and methylated
634 using a fatty acid methylation kit (06482-04, Nacalai Tesque) and then purified using a fatty acid
635 methyl ester purification kit (06483-94, Nacalai Tesque). The methylated sample (3.0 mL) was
636 dried and dissolved in 50 μL of elution solution. Samples were subjected to GC-MS.
637 Fatty acids were determined on an Agilent 7890A GC system coupled with a JMS-T 100 GCv
638 mass detector at the Natural Science Research Center, Hiroshima University (N-BARD). Sample
639 (1.0 μL aliquot) was injected to SP®-2560 capillary GC column (100 m × 0.25 mm i.d. × 0.2 μm
640 film thickness; 24056, Sigma-Aldrich). For measurements, helium was used as the carrier gas at
641 a constant flow rate of 2.0 mL/min. The GC oven temperature was gradually increased from
642 100°C to 300°C at a rate of 10°C/min and held at 300°C for 20 minutes. Ionization was performed
643 using electron ionization with an electron energy of 70 eV. Mass spectra were obtained in scan
644 mode (mass scan range 29-800 m/z). NIST MS Search v.2.0 was used to detect and identify of
645 fatty acids.
646
647 **Sperm motility parameters with the lipid Mixture**
648 Sperm recovered from the cauda epididymis of male mice were dispersed in 500 μL of mHTF
649 without BSA and centrifuged at 300 × g for 3 minutes to wash out epididymis-derived factors.
650 The sperm pellets were resuspended in HTF medium with or without a lipid mixture (LM) that
651 included 2 μg/mL arachidonic acid, 10 μg/mL linoleic acid, 10 μg/mL linolenic acid, 10 μg/mL
652 myristic acid, 10 μg/mL oleic acid, 10 μg/mL palmitic acid, and 10 μg/mL stearic acid (L0288,
653 Sigma-Aldrich). The sperm were then incubated for 60 minutes at 37°C under a humidified
654 atmosphere of 5% CO2. Sperm motility patterns were subsequently examined using CASA.
655
656 **ACLY knock down experiment using shRNA**

657 The U6 shRNA lentiviral vector of the *Acly* gene (mAcly[shRNA#1]; a virus packaging service,
658 VectorBuilder, Chicago, IL, USA) was used for knockdown experiments. The ACLY sequence
659 targeted by the shRNA vector used in this study was 5′-GCAGCAAAGATGTTCAGTAAA-3′.
660 Lentivirally transduced cells were prepared according to manufacture protocol. Immediately after
661 isolation, the mouse seminal vesicle epithelial cells were cultured overnight in a medium
662 containing 5 μg/mL polybrene (VectorBuilder) and lentiviral particles expressing an shRNA
663 targeting ACLY or a scramble (Multiplicity of Infection of 10). After an additional overnight
664 incubation in a fresh culture medium, the cells were incubated for 5 days in a medium containing
665 1 μg/ml puromycin (19752-64, Nacalai tesque). 100 ng/mL of testosterone was added to all
666 procedures for the testosterone-treated group. Infection efficiency, calculated based on the
667 number of GFP-positive cells using an APX100 Digital Imaging System, ranged between 70%
668 and 90%.
669 For sperm motility analysis, sperm were collected and washed with mHTF from the culture
670 supernatant and cauda epididymis. The samples were incubated at 37°C for 60 minutes in a
671 humidified atmosphere of 5% CO2 in air. The sperm motility pattern was then examined using
672 CASA.
673
674 **Western blot analysis**
675 Protein samples of mouse seminal vesicle epithelial cells, seminal vesicle tissue, and sperm
676 were prepared by homogenization in cell lysis buffer (04719964001, cOmplete™ Lysis-M
677 EDTA-free, Roche) and diluted with an equal volume of sample buffer solution containing 2-ME
678 (2 ×) for SDS-PAGE (30566-22, Nacalai tesque). The extracts (10 μg protein) were separated by
679 SDS-polyacrylamide gel (10%) electrophoresis and transferred to polyvinylidene fluoride
680 membranes (10600069, Cytiva, Tokyo, Japan). The membranes were then treated with Tris-
681 buffered saline and Tween 20 (TBST, 20 mM Tris, pH 7.5, 150 mM NaCl, 0.1% Tween 20)
682 containing 5% (w/v) Non-Fat Dry milk (MORINAGA MILK INDUSTRY Co., Ltd., Tokyo,
683 Japan) for the nonspecific reaction was blocked. The membranes were incubated overnight at 4°C
684 with primary antibodies: anti-GLUT4 antibody (1:100; ab33780; Abcam), anti-ACLY antibody
685 (1:10,000; ab40793; Abcam) or anti-α/β-Tubulin antibody (1:1,000; 2148S; Cell Signaling). The
686 next day, membranes were washed with TBST and incubated with HRP-labeled antibody specific

687 for rabbit IgG (1:4000; 7074S; Cell Signaling). The bands were visualized by using Enhanced
688 Chemiluminescence detection systems (RPN2232, Cytiva) and ChemiDoc™ MP Imaging System
689 (BIO-RAD Laboratories). The bands were analyzed by using the software ImageJ. Densitometry
690 analysis was performed using the ImageJ Gel Analysis tool, and the background of the gel was
691 also removed individually for each band. The full-length blotting images are shown in
692 Supplementary Figure 7.
693
694 **Statistical analysis**
695 Quantitative data were presented as means ± SEM. The Bartlett's test was used to confirm
696 whether the variances were equal for each group in experiments consisting of three or more
697 groups. All statistical details of the experiments are given in the figure legends. R [(version
698 4.3.1 (2023-06-16)] was used for statistical analysis. Data were considered statistically
699 significant at $p < 0.05$.
700
701 **Data availability**
702 Nucleotide sequence data reported are available in the DDBJ Sequenced Read Archive under
703 the accession numbers DRA017090. Additional information needed to reanalyze the data
704 reported in this paper is available from the principal contact upon request.
705
706 **List of Supplementary Materials**
707 Supplemental Figures 1 to 8
708 Table S1
709
710 **Acknowledgments:**
711 The authors would like to thank JoAnne S. Richards for carefully proofreading the manuscript
712 and useful comments.
713
714 **Funding:**
715 This work was supported in part by JSPS KAKENHI Grant Number 23K14069 to TU and
716 23H00361 to MS.

Author contributions:

Conceptualization: TY, TU, MS

Methodology: TY, ZX, NT, MA, TU

Investigation: TY, ZX, NT, MA, TU

Visualization: TY, MS

Funding acquisition: TU, MS

Supervision: MS

Writing – original draft: TY

Writing – review & editing: TY, TU, MS

Competing interests:

MS holds stocks in and receives a salary from Hiroshima Cryopreservation Service Co. as a director. In addition, MS has received royalties and grants from Hiroshima Cryopreservation Service Co. M.S. has received consulting fees from Rohto Pharmaceutical Co., Ltd.. TU holds stocks in and receives a salary from Lullabio Inc. as a director and has received honoraria from Rohto Pharmaceutical Co., Ltd. The other authors declare they have no competing interests.

References

1. World Health Organization., Infertility prevalence estimates: 1990–2021. *Global report* , 1–98 (2023).

2. S. A. Kidd, B. Eskenazi, A. J. Wyrobek, Effects of male age on semen quality and fertility: a review of the literature. *Fertil Steril* **75**, 237–248 (2001).

3. A. Mumcu, A. Karaer, B. Dogan, G. Tuncay, Metabolomics analysis of seminal plasma in patients with idiopathic Oligoasthenoteratozoospermia using high-resolution NMR spectroscopy. *Andrology* **8**, 450–456 (2020).

4. Y. Xu, H. Lu, Y. Wang, Z. Zhang, Q. Wu, Comprehensive metabolic profiles of seminal plasma with different forms of male infertility and their correlation with sperm parameters. *J Pharm Biomed Anal* **177**, 112888 (2020)

5. S. Elbashir, Y. Magdi, A. Rashed, R. Henkel, A. Agarwal, Epididymal contribution to male

747 infertility: An overlooked problem. *Andrologia* **53**, e13721 (2021).
748 6. M. J. Cosentino, A. T. K. Cockett, Review Article: Structure and Function of the Epididymis
749 Transport of Spermatozoa. *Urol Res* **14**, 229–240 (1986).
750 7. B. Howarth, Fertilizing ability of cock spermatozoa from the testis epididymis and vas deferens
751 following intramagnal insemination. *Biol Reprod* **28**, 586–590 (1983).
752 8. R. Yanagimachi, The movement of golden hamster spermatozoa before and after capacitation.
753 *J Reprod Fertil* **23**, 193–196 (1970).
754 9. R. Yanagimachi, Mammalian Fertilization. E. Knobil, J.D. Neill (Eds.), *The physiology of*
755 *reproduction*, Raven Press, 189–317 (1994).
756 10. P. Gaddum-Rosse, Some observations on sperm transport through the uterotubal junction of
757 the rat. *Am J Anat* **160**, 333–341 (1981).
758 11. R. Shalgi, T. T. Smith, R. Yanagimachi2, A Quantitative Comparison of the Passage of
759 Capacitated and Uncapacitated Hamster Spermatozoa through the Uterotubal Junction. *Biol*
760 *Reprod* **46**, 419–424 (1992).
761 12. H. Li, P. Hung, S. S. Suarez, Ejaculated Mouse Sperm Enter Cumulus-Oocyte Complexes
762 More Efficiently In Vitro than Epididymal Sperm. *PLoS One* **10**, e0127753 (2015)
763 13. T. Noda, M. Ikawa, Physiological function of seminal vesicle secretions on male fecundity.
764 *Reprod Med Biol* **18**, 241–246 (2019).
765 14. P. Verze, T. Cai, S. Lorenzetti, The role of the prostate in male fertility, health and disease. *Nat*
766 *Rev Urol* **13**, 379–386 (2016).
767 15. E. Balandya, W. Wieland-Alter, K. Sanders, T. Lahey, Human Seminal Plasma Fosters CD4+
768 Regulatory T-cell Phenotype and Transforming Growth Factor-β1 Expression. *American Journal*
769 *of Reproductive Immunology* **68**, 322–330 (2012).
770 16. T. Shima, K. Inada, A. Nakashima, A. Ushijima, M. Ito, O. Yoshino, S. Saito, Paternal antigen-
771 specific proliferating regulatory T cells are increased in uterine-draining lymph nodes just before
772 implantation and in pregnant uterus just after implantation by seminal plasma-priming in
773 allogeneic mouse pregnancy. *J Reprod Immunol* **108**, 72–82 (2015).
774 17. N. Kawano, N. Araki, K. Yoshida, T. Hibino, N. Ohnami, M. Makino, S. Kanai, H. Hasuwa,
775 M. Yoshida, K. Miyado, A. Umezawa, Seminal vesicle protein SVS2 is required for sperm
776 survival in the uterus. *Proc Natl Acad Sci U S A* **111**, 4145–4150 (2014).

18. R. R. Rosecrans, R. S. Jeyendran, M. Perez-Pelaez, W. P. Kennedy, Comparison of Biochemical Parameters of Human Blood Serum and Seminal Plasma. *Andrologia* **19**, 625–628 (1987).

19. T. Umehara, T. Kawai, M. Goto, J. A. S. Richards, M. Shimada, Creatine enhances the duration of sperm capacitation: a novel factor for improving in vitro fertilization with small numbers of sperm. *Human Reproduction* **33**, 1117–1129 (2018).

20. Z. Zhu, T. Kawai, T. Umehara, S. A. M. Hoque, W. Zeng, M. Shimada, Negative effects of ROS generated during linear sperm motility on gene expression and ATP generation in boar sperm mitochondria. *Free Radic Biol Med* **141**, 159–171 (2019).

21. M. M. Islam, T. Umehara, N. Tsujita, M. Shimada, Saturated fatty acids accelerate linear motility through mitochondrial ATP production in bull sperm. *Reprod Med Biol* **20**, 289–298 (2021).

22. T. Noda, Y. Fujihara, T. Matsumura, S. Oura, S. Kobayashi, M. Ikawa, Seminal vesicle secretory protein 7, PATE4, is not required for sperm function but for copulatory plug formation to ensure fecundity. *Biol Reprod* **100**, 1035–1045 (2019).

23. K. Queen, C. B. Dhabuwala, C. G. Pierrepoint, The effect of the removal of the various accessory sex glands on the fertility of male rats. *J Reprod Fertil* **62**, 423–426 (1981).

24. Mann T, Studies on the metabolism of semen; fructose as a normal constituent of seminal plasma; site of formation and function of fructose in semen. *Biochem J* **40**, 481–491 (1946).

25. Humphrey GF, Mann T, Studies on the metabolism of semen; citric acid in semen. *Biochem J* **44**, 97–105 (1949).

26. C. Chang, S. O. Lee, R. S. Wang, S. Yeh, T. M. Chang, Androgen receptor (AR) physiological roles in male and female reproductive systems: lessons learned from AR-knockout mice lacking AR in selective cells. *Biol Reprod* **89**, 1–16 (2013).

27. C. Fix, C. Jordan, P. Cano, W. H. Walker, Testosterone activates mitogen-activated protein kinase and the cAMP response element binding protein transcription factor in Sertoli cells. *Proc Natl Acad Sci U S A* **101**, 10919–10924 (2004).

28. K. Nagaosa, A. Kishimoto, R. Kizu, A. Nakagawa, A. Shiratsuchi, Y. Nakanishi, Perturbation of spermatogenesis by androgen antagonists directly injected into seminiferous tubules of live mice. *Reproduction* **133**, 21–27 (2007).

807 29. L. B. Smith, W. H. Walker, The regulation of spermatogenesis by androgens. *Semin Cell Dev*
808 *Biol* **30**, 2–13 (2014).
809 30. P. S. Cooke, W. H. Walker, Male fertility in mice requires classical and nonclassical androgen
810 signaling. *Cell Rep* **36**, 109557 (2021).
811 31. S. P. Smyth, B. Nixon, A. L. Anderson, H. C. Murray, J. H. Martin, L. A. MacDougall, S. A.
812 Robertson, D. A. Skerrett-Byrne, J. E. Schjenken, Elucidation of the protein composition of
813 mouse seminal vesicle fluid. *Proteomics* **22**, e2100227 (2022).
814 32. H. Murata, P. W. Hruz, M. Mueckler, Indinavir inhibits the glucose transporter isoform Glut4
815 at physiologic concentrations. *AIDS* **16**, 859–863 (2002).
816 33. C. Wilson, A. Contreras-Ferrat, N. Venegas, C. Osorio-Fuentealba, M. Pávez, K. Montoya, J.
817 Durán, R. Maass, S. Lavandero, M. Estrada, Testosterone increases GLUT4-dependent glucose
818 uptake in cardiomyocytes. *J Cell Physiol* **228**, 2399–2407 (2013).
819 34. G. F. Gonzales, Function of seminal vesicles and their role on male fertility. *Asian J Androl* **3**,
820 251–258 (2001).
821 35. A. Lenzi, M. Picardo, L. Gandini, F. Dondero, Lipids of the sperm plasma membrane: from
822 polyunsaturated fatty acids considered as markers of sperm function to possible scavenger therapy.
823 *Hum Reprod Update* **2**, 246–256 (1996).
824 36. M. T. Haren, A. M. Siddiqui, H. J. Armbrecht, R. T. Kevorkian, M. J. Kim, M. J. Haas, A.
825 Mazza, V. B. Kumar, M. Green, W. A. Banks, J. E. Morley, Testosterone modulates gene
826 expression pathways regulating nutrient accumulation, glucose metabolism and protein turnover
827 in mouse skeletal muscle. *Int J Androl* **34**, 55–68 (2011).
828 37. L. C. Costello, R. B. Franklin, Testosterone and prolactin regulation of metabolic genes and
829 citrate metabolism of prostate epithelial cells. *Horm Metab Res* **34**, 417–424 (2002).
830 38. K. Gonthier, R. T. K. Poluri, É. Audet-Walsh, Functional genomic studies reveal the androgen
831 receptor as a master regulator of cellular energy metabolism in prostate cancer. *J Steroid Biochem*
832 *Mol Biol* **191**, 105367 (2019).
833 39. M. F. Troncoso, M. Pavez, C. Wilson, D. Lagos, J. Duran, S. Ramos, G. Barrientos, P. Silva,
834 P. Llanos, C. Basualto-Alarcón, B. D. Westenbrink, S. Lavandero, M. Estrada, Testosterone
835 activates glucose metabolism through AMPK and androgen signaling in cardiomyocyte
836 hypertrophy. *Biol Res* **54**, 1–16 (2021).

837 40. Chen X, Li X, Huang HY, Li X, Lin JF, Effects of testosterone on insulin receptor substrate-
838 1 and glucose transporter 4 expression in cells sensitive to insulin. *Zhonghua Yi Xue Za Zhi* **86**,
839 1474–1477 (2006).
840 41. K. Sato, M. Iemitsu, K. Aizawa, R. Ajisaka, Testosterone and DHEA activate the glucose
841 metabolism-related signaling pathway in skeletal muscle. *Am J Physiol Endocrinol Metab* **294**,
842 E961–E968 (2008).
843 42. P. K. Arnold, B. T. Jackson, K. I. Paras, J. S. Brunner, M. L. Hart, O. J. Newsom, S. P.
844 Alibeckoff, J. Endress, E. Drill, L. B. Sullivan, L. W. S. Finley, A non-canonical tricarboxylic acid
845 cycle underlies cellular identity. *Nature* **603**, 477–481 (2022).
846 43. A. Luengo, Z. Li, D. Y. Gui, L. B. Sullivan, M. Zagorulya, B. T. Do, R. Ferreira, A. Naamati,
847 A. Ali, C. A. Lewis, C. J. Thomas, S. Spranger, N. J. Matheson, M. G. Vander Heiden, Increased
848 demand for NAD+ relative to ATP drives aerobic glycolysis. *Mol Cell* **81**, 691–707 (2021).
849 44. B. B. Yeap, Testosterone and cardiovascular disease risk. *Curr Opin Endocrinol Diabetes*
850 *Obes* **22**, 193–202 (2015).
851 45. J. D. Marsh, M. H. Lehmann, R. H. Ritchie, J. K. Gwathmey, G. E. Green, R. J. Schiebinger,
852 Androgen receptors mediate hypertrophy in cardiac myocytes. *Circulation* **98**, 256–261 (1998).
853 46. G. F. Grabner, H. Xie, M. Schweiger, R. Zechner, Lipolysis: cellular mechanisms for lipid
854 mobilization from fat stores. *Nat Metab* **3**, 1445–1465 (2021).
855 47. B. Mittendorfer, Origins of metabolic complications in obesity: adipose tissue and free fatty
856 acid trafficking. *Curr Opin Clin Nutr Metab Care* **14**, 535–541 (2011).
857 48. H. Wackerhage, I. J. Vechetti, P. Baumert, S. Gehlert, L. Becker, R. T. Jaspers, M. H. de
858 Angelis, Does a Hypertrophying Muscle Fibre Reprogramme its Metabolism Similar to a Cancer
859 Cell? *Sports Med* **52**, 2569–2578 (2022).
860 49. R. J. De Berardinis, N. S. Chandel, Fundamentals of cancer metabolism. *Sci Adv* **2**, e1600200
861 (2016).
862 50. G. L. Semenza, Hypoxia-inducible factors in physiology and medicine. *Cell* **148**, 399–408
863 (2012).
864 51. B. Morant-Ferrando, D. Jimenez-Blasco, P. Alonso-Batan, J. Agulla, R. Lapresa, D. Garcia-
865 Rodriguez, S. Yunta-Sanchez, I. Lopez-Fabuel, E. Fernandez, P. Carmeliet, A. Almeida, M.
866 Garcia-Macia, J. P. Bolaños, Fatty acid oxidation organizes mitochondrial supercomplexes to

867 sustain astrocytic ROS and cognition. *Nat Metab* **5**, 1290–1302 (2023).
868 52. M. Duta-Mare, V. Sachdev, C. Leopold, D. Kolb, N. Vujic, M. Korbelius, D. C. Hofer, W. Xia,
869 K. Huber, M. Auer, B. Gottschalk, C. Magnes, W. F. Graier, A. Prokesch, B. Radovic, J. G.
870 Bogner-Strauss, D. Kratky, Lysosomal acid lipase regulates fatty acid channeling in brown
871 adipose tissue to maintain thermogenesis. *Biochim Biophys Acta Mol Cell Biol Lipids* **1863**, 467–
872 478 (2018).
873 53. S. C. C. Huang, B. Everts, Y. Ivanova, D. O'Sullivan, M. Nascimento, A. M. Smith, W. Beatty,
874 L. Love-Gregory, W. Y. Lam, C. M. O'Neill, C. Yan, H. Du, N. A. Abumrad, J. F. Urban, M. N.
875 Artyomov, E. L. Pearce, E. J. Pearce, Cell-intrinsic lysosomal lipolysis is essential for alternative
876 activation of macrophages. *Nat Immunol* **15**, 846–855 (2014).
877 54. K. H. Tsui, T. H. Feng, Y. F. Lin, P. L. Chang, H. H. Juang, p53 downregulates the gene
878 expression of mitochondrial aconitase in human prostate carcinoma cells. *Prostate* **71**, 62–70
879 (2011).
880 55. S. Almeida, L. Rato, M. Sousa, M. G. Alves, P. F. Oliveira, Fertility and Sperm Quality in the
881 Aging Male. *Curr Pharm Des* **23**, 4429–4437 (2017).
882 56. T. Murata, Y. Ishitsuka, K. Karouji, H. Kaneda, H. Toki, Y. Nakai, S. Makino, R. Fukumura,
883 H. Kotaki, S. Wakana, T. Noda, Y. Gondo, β-cateninC429S mice exhibit sterility consequent to
884 spatiotemporally sustained Wnt signalling in the internal genitalia. *Sci Rep* **4**, 6959 1–7 (2014).
885 57. B. A. Stone, A. Alex, L. B. Werlin, R. P. Marrs, Age thresholds for changes in semen
886 parameters in men. *Fertil Steril* **100**, 952–958 (2013).
887 58. J. L. Frattarelli, K. A. Miller, B. T. Miller, K. Elkind-Hirsch, R. T. Scott, Male age negatively
888 impacts embryo development and reproductive outcome in donor oocyte assisted reproductive
889 technology cycles. *Fertil Steril* **90**, 97–103 (2008).
890 59. A. P. Drabovich, P. Saraon, K. Jarvi, E. P. Diamandis, Seminal plasma as a diagnostic fluid
891 for male reproductive system disorders. *Nat Rev Urol* **11**, 278–288 (2014).
892 60. T. Umehara, N. Tsujita, Z. Zhu, M. Ikedo, M. Shimada, A simple sperm-sexing method that
893 activates TLR7/8 on X sperm for the efficient production of sexed mouse or cattle embryos. *Nat*
894 *Protoc* **15**, 2645–2667 (2020).
895 61. C. Prieto, D. Barrios, RaNA-Seq: Interactive RNA-Seq analysis from FASTQ files to
896 functional analysis. *Bioinformatics* **36**, 1955–1956 (2019).

Figures and Figure legends

Fig.1

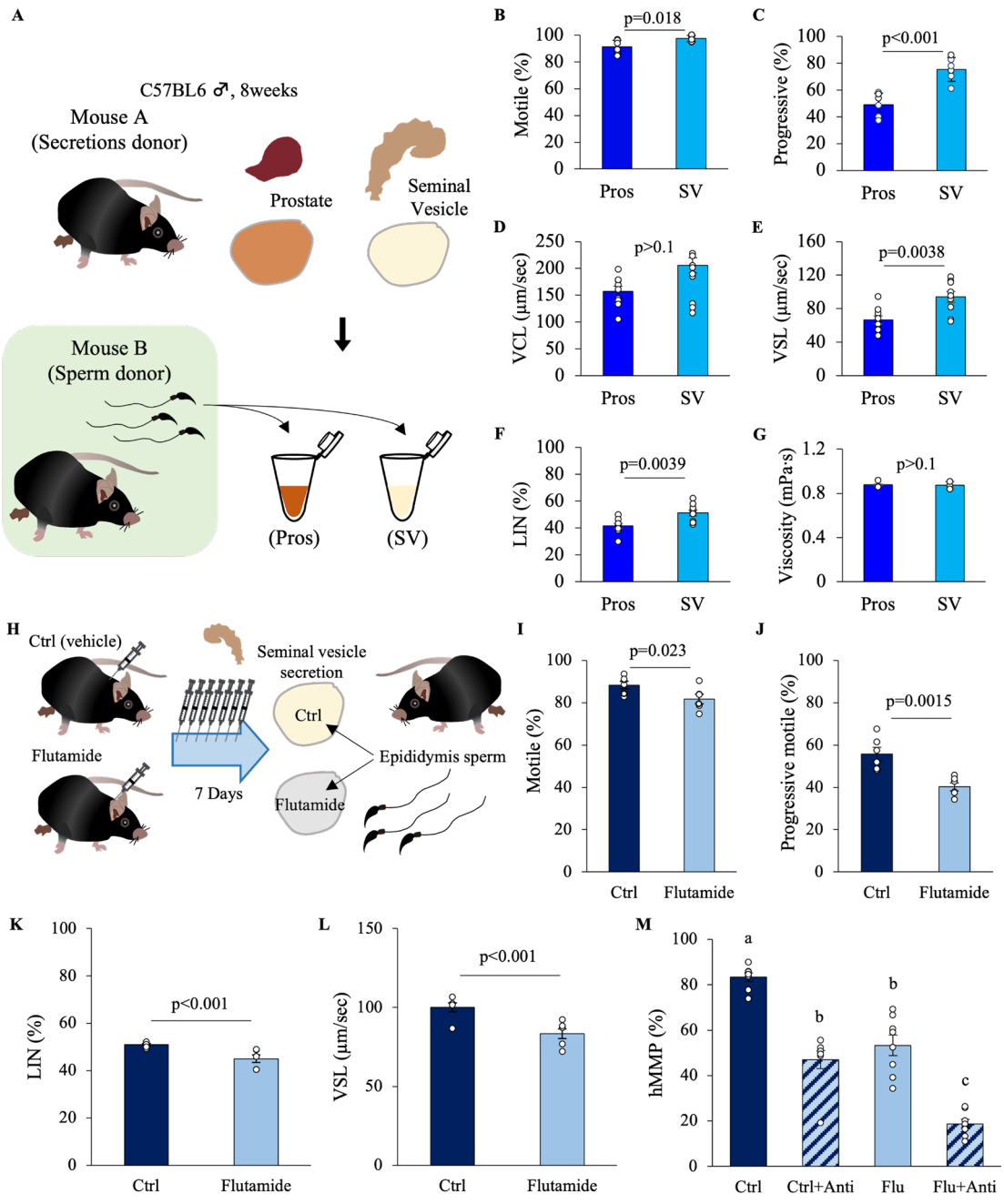

Figure 1. Effects of seminal vesicle fluid and prostate fluids on sperm motility (A) The effects of secretions from the prostate and seminal vesicles on sperm motility were directly compared. (B-F) The effects of secretions from the prostate (Pros) or seminal vesicles (SV) on the motility parameters of epididymal sperm were tested: (B) Motile, (C) Progressive motile, (D) Curvi-Linear Velocity; VCL, (E) Straight-Line Velocity; VSL and (F) Linearity; LIN is the ratio of VSL

914 to VCL of sperm that was incubated with the mixture of seminal vesicle secretions or prostate
915 extracts. (G) Viscosity of a solution containing prostate or seminal vesicle secretion with a protein
916 concentration of 10 mg/mL. (H) Experimental design to evaluate the effect of seminal vesicle
917 secretions collected from male mice treated with or without flutamide (50 mg/kg subcutaneously
918 every day for 7 days) on sperm. Note that the donor mice for sperm and seminal vesicle secretions
919 were different. (I-L) Performed bioassay using seminal vesicle fluid after treatment with vehicle
920 (Ctrl) or flutamide: (I) Motile, (J) Progressive motile, (K) LIN, (L) VSL. (M) The high
921 mitochondrial membrane potential (hMMP) was checked by the JC-1 kit. Antimycin (Anti) was
922 used as the negative control for hMMP. Data are mean ± SEM. n=3-9 independent replicates. The
923 viscosity measurement data were from n=3 repeated experiments using pooled prostate or seminal
924 vesicle extracts from at least 20 mice. Percentage data were subjected to arcsine transformation
925 before statistical analysis. (B-G, I-L) Significance was tested in comparison using Student's t-test.
926 (M) Since the results of the Bartlett test were significant, a two-way ANOVA using a generalized
927 linear model was performed. Both the flutamide administration and antimycin addition were
928 significant. The interaction was not significant. Games-Howell was performed as a post hoc test.
929 Different letters represent significantly different groups.
930
931
932

933 **Fig.2**

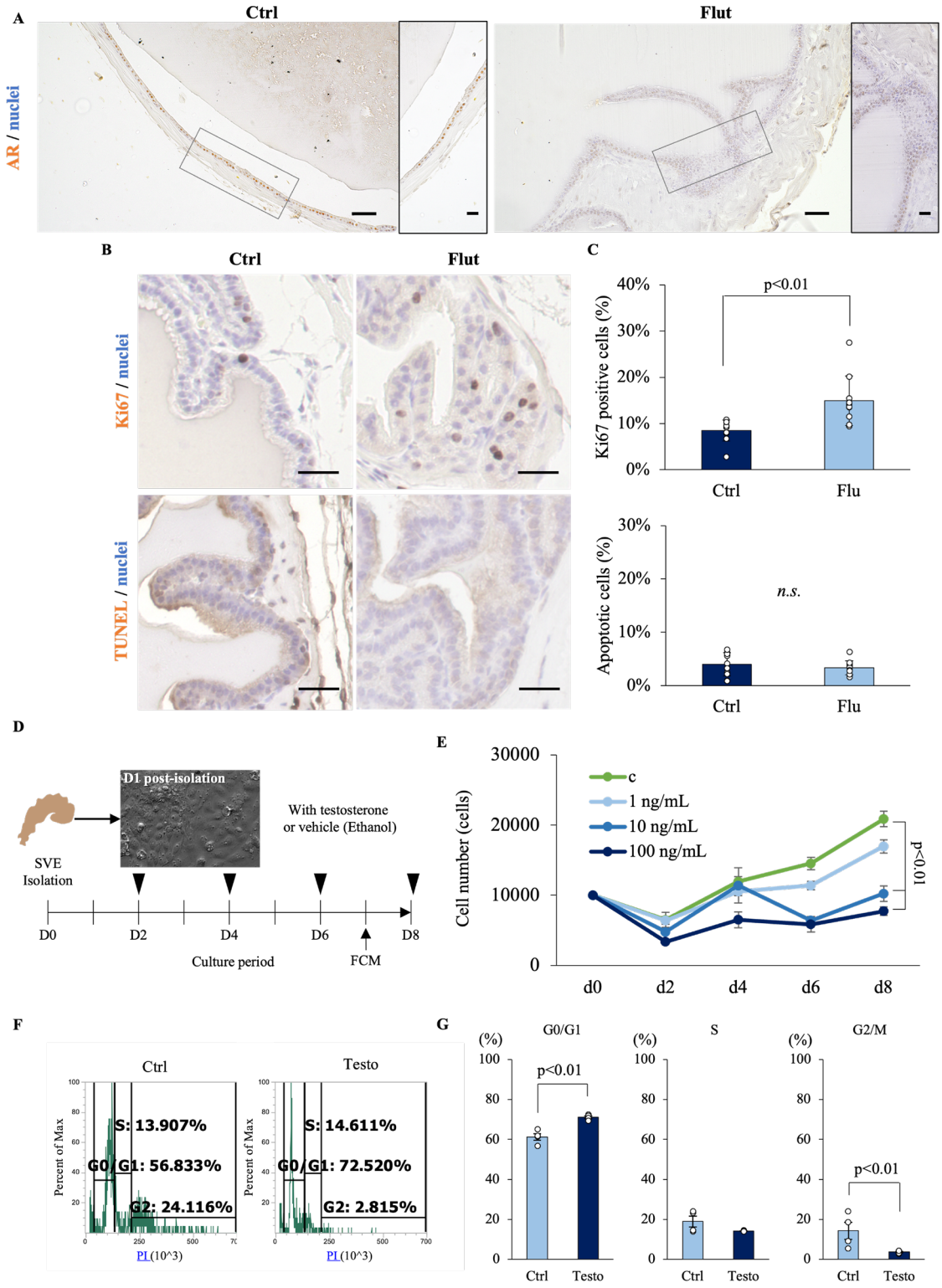

934

935

936 **Figure 2. The testosterone-androgen receptor pathway inhibits the cell proliferation of**
937 **seminal vesicle epithelial cells.** (A) The localization of the androgen receptor (AR; NR3C4) in
938 seminal vesicle of control (Ctrl) mice and those treated with flutamide (Fult). Scale bar=50 μm
939 from 10× magnification for left panel and 20 μm from 20× magnification for right panel in each
940 group. (B,C) Cell proliferation and apoptosis in seminal vesicle of control (Ctrl) mice and those
941 treated with flutamide (Fult): (B) Representative images of Ctrl and Flut staining for Ki67 (top)
942 and TUNEL (bottom). Scale bar=20 μm. (C) Percentage of Ki67 positive cells (top) and TUNEL
943 positive (bottom) in Ctrl and Flut-treated seminal vesicle sections. (D) Experimental design to
944 evaluate the effects of testosterone on the proliferation of seminal vesicle epithelial cells *in vitro*.
945 The epithelial cells were culutured with or without testosterone for 8 days. (E) Growth curves of
946 seminal vesicle epithelial cells that cultured with 0 (c), 1, 10 and 100 ng/mL of testosterone. (F,G)
947 Cell cycle status was determined by flow cytometry. Data are mean ± SEM. n=3-5 mice or
948 independent replicates. Each replicate experiments with 3-6 wells containing pooled cells from
949 3-5 mice. Percentage data were subjected to arcsine transformation before statistical analysis.
950 Significance was tested in comparison to Ctrl using Student's t-test. The cell number data at d8
951 was compared with the control using Dunnett's test.
952
953

954 **Fig.3**

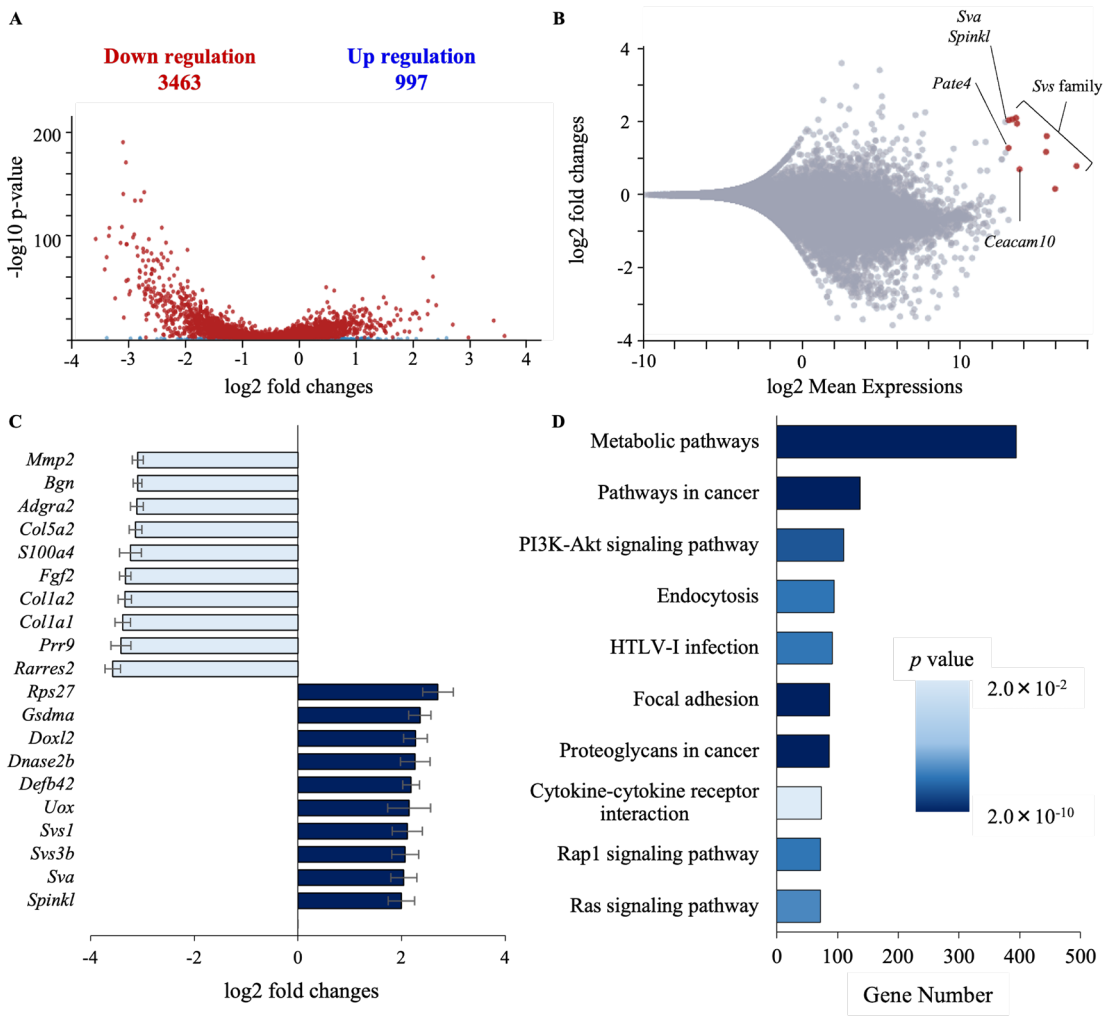

955

956 **Figure 3. Testosterone changes the expression of genes involved in metabolic pathway in**
957 **seminal vesicle epithelial cells.** (A) Volcano plot of differentially expressed genes. RNA
958 sequencing was performed using RNA extracted from the seminal vesicle epithelial cells cultured
959 with or without 100 ng/mL testosterone. Genes with a significant expression change are
960 highlighted as red dots. It found 4460 significant genes for a cutoff of P<0.05. (B) MA plot of
961 differential expression results. The seminal vesicle specific genes are highlighted as red dots
962 rather than significant genes. (C) Top 10 genes upregulated or downregulated by testosterone,
963 respectively, for altered gene expression. (D) Conducted KEGG analysis to identify differences
964 in pathway enrichment by testosterone, identifying the most variability in metabolic pathway
965 genes. It shows the number of differential expressed genes annotated to Gene Ontology shows (x

axis). p-value which measure the statistical significance of a possible functional enrichment for each term.

969 **Fig.4**

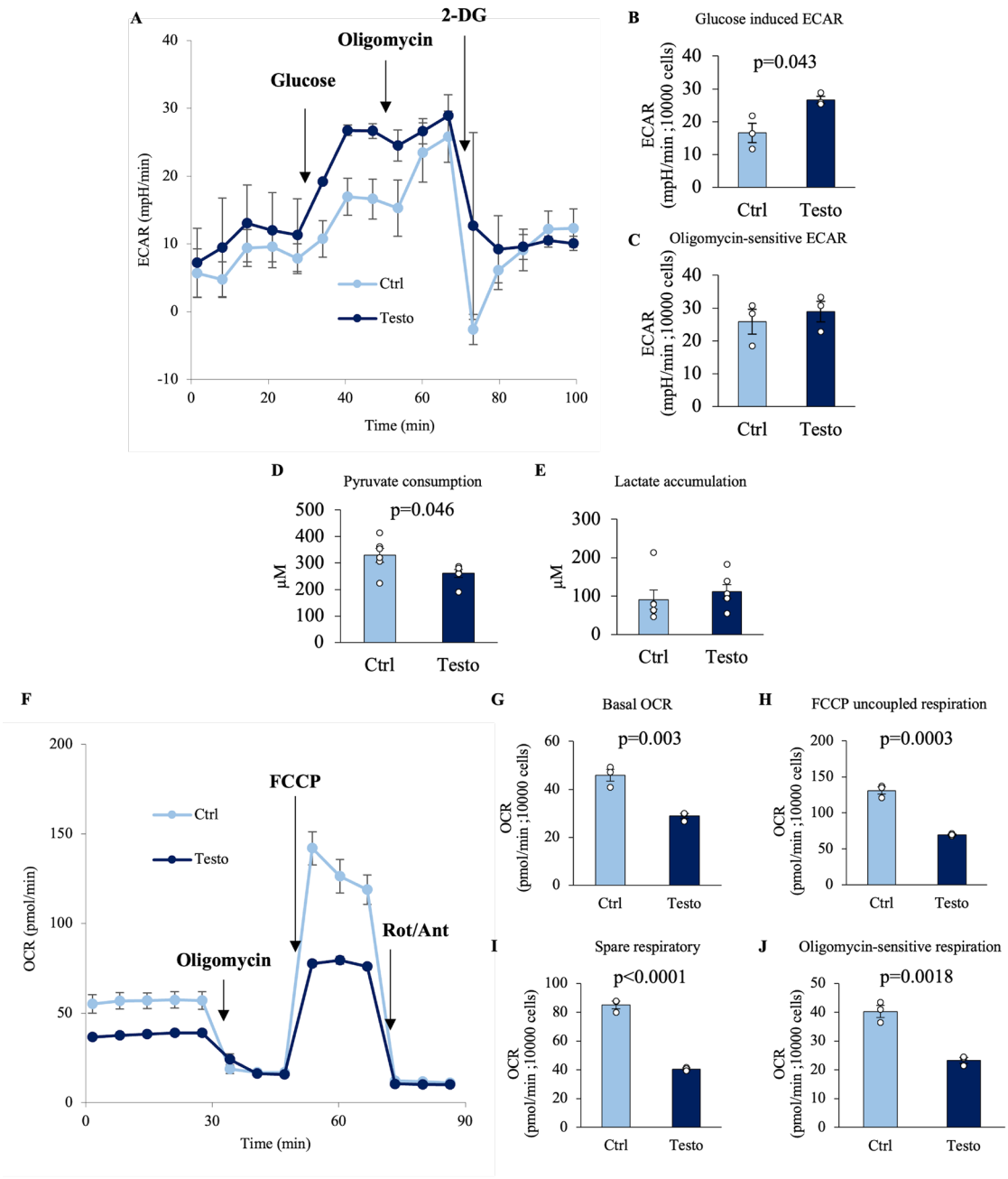

970

971 **Figure 4. Testosterone regulates glucose metabolism and mitochondrial ATP production in**
972 **seminal vesicle epithelial cells.** (A-C) Extracellular acidification rate (ECAR) analysis by an
973 extracellular flux analyzer in seminal vesicle epithelial cells cultured with 100 ng/mL
974 testosterone (Testo) or vehicle (Ctrl) for 7 days: (A) ECAR kinetics of seminal vesicle epithelial
975 cells using an extracellular flux analyzer. (B) Glucose induced ECAR and (C) Oligomycin-
976 sensitive ECAR. (D,E) The concentrations of pyruvate and lactate in the culture supernatant.

977 These measurements were normalized based on cell count and viability. (D) Pyruvate
978 concentration in the medium where seminal vesicle epithelial cells were cultured with or
979 without testosterone for 24 hours. (E) Lactate concentration. (F-J) Mitochondrial respiration
980 measurement by an extracellular flux analyzer: (F) Oxygen consumption rate (OCR) kinetics of
981 seminal vesicle epithelial cells with or without 100 ng/mL testosterone. (G) Basal OCR, (H)
982 FCCP uncoupled respiration, (I) Spare respiratory capacity and (J) Oligomycin-sensitive
983 respiration. Data are mean ± SEM of n = 3 replicate experiments with 3-6 wells containing
984 pooled cells from 3-5 mice or medium. Student's t-test was used to compare Ctrl and Testo. The
985 cells were normalized to 10,000 viable cells/well immediately before analysis. The viability of
986 the cells before experiments was 86-93%.
987

988 **Fig.5**

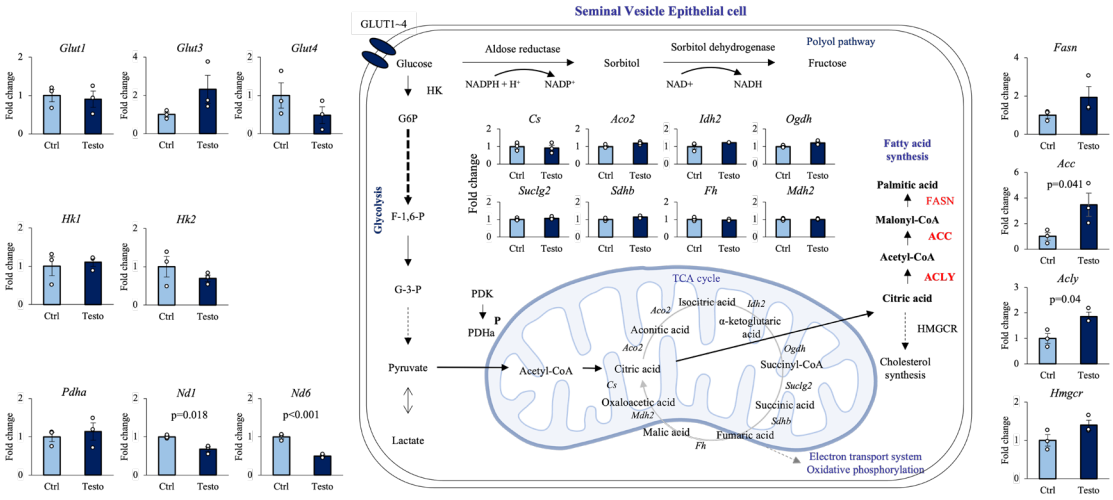

989

990 **Figure 5. Effect of testosterone on gene expression of enzymes involved in the glucose**
991 **metabolic pathway in seminal vesicle epithelial cells.** To elucidate the effects of testosterone
992 on gene expression of enzymes involved in glucose catabolism and anabolism in seminal vesicle
993 epithelial cells. ctrl: 7 days of culture with vehicle. Testo: 7 days of culture with 100 ng/mL
994 testosterone. Data are mean ± SEM of n = 3 replicate experiments with 3-6 wells containing
995 pooled cells from 3-5 mice. Student's t-test was used to compare Ctrl and Testo.

996

997

998 **Fig.6**

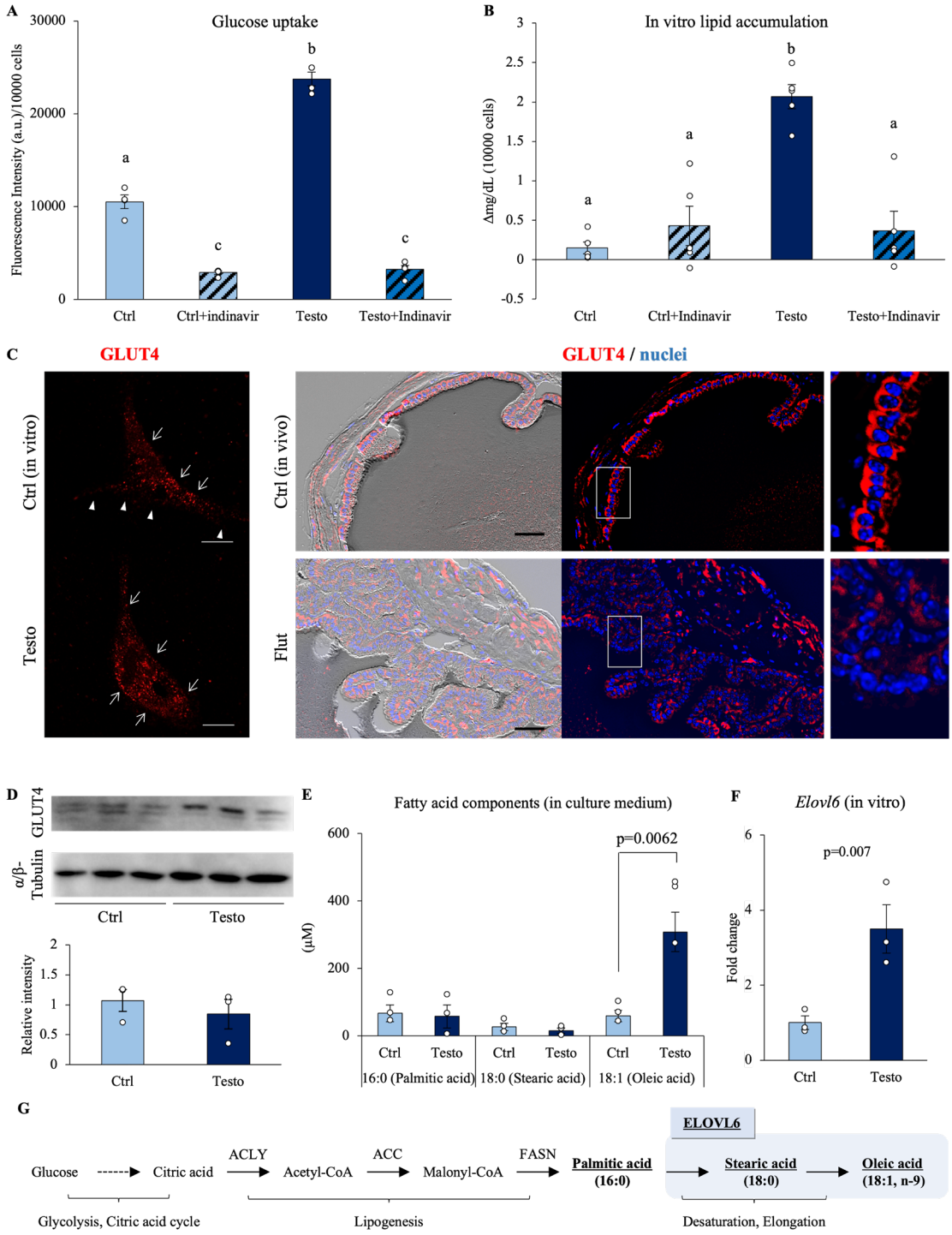

999

1000 **Fig.6 Testosterone enhances glucose uptake and fatty acid synthesis via GLUT4 trans-**
1001 **localization in seminal vesicle epithelial cells.** (A) The glucose uptake ability of seminal vesicle
1002 epithelial cells was detected using fluorescence-tagged glucose. The cells were cultured with 100

1003 ng/mL testosterone and/or indinavir (100 μM) for 7 days and then further treated with glucose
1004 uptake probe-green for 15 min, and intracellular fluorescence was measured by flow cytometry
1005 (n=4). (B) Lipid accumulation in the medium where seminal vesicle epithelial cells were
1006 incubated for 24 hours (n=6). (C) Immunostaining of GLUT4 in flutamide-treated or vehicle mice
1007 derived seminal vesicle. Scale bar is 50 μm. (D) Western blot images of GLUT4 and α/β-tubulin
1008 in three sets of seminal vesicle epithelial cells cultured with 100 ng/mL testosterone (Testo) or in
1009 vehicle (Ctrl) for 7 days. Quantitative analysis of GLUT4 relative to α-tubulin obtained from
1010 Western blot. (E) Fatty acid composition in the medium was analyzed using gas chromatography.
1011 (F) Quantification of *Elovl* family gene expression by RT-qPCR. (G) Pathway of glucose
1012 assimilation to oleic acid. Data are mean ± SEM. n=3-6 independent replicates. Each replicate
1013 experiments with 3-6 wells containing pooled cells from 3-5 mice or medium. (A,B) The glucose
1014 uptake and lipid measurements were normalized based on cell count and viability. A two-way
1015 ANOVA was performed. Both the Indinavir and testosterone treatment were significant. The
1016 interaction was significant. Tukey's Honest Significant Difference test was performed as a post
1017 hoc test. Different letters represent significantly different groups. Student's t-test was used for
1018 comparison between the two groups.
1019
1020
1021
1022
1023
1024
1025
1026
1027

1028 **Fig.7**

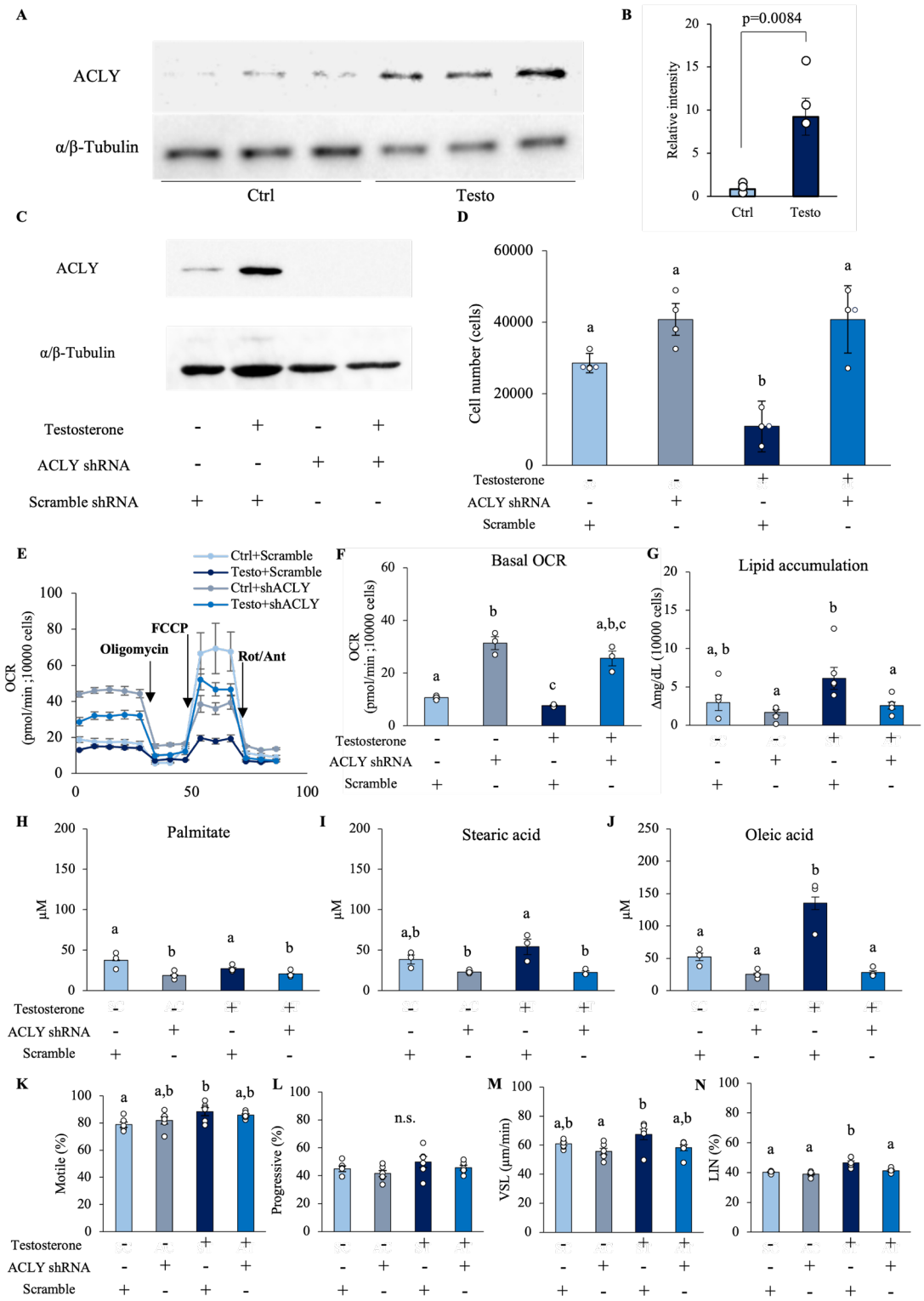

1029

1030 **Figure 7. Testosterone-regulated ACLY induces metabolic shifts in seminal vesicle epithelial**

1031 **cells.** (A) Western blot images of ACLY and α/β-tubulin in three sets of seminal vesicle epithelial

1032 cells cultured with 100 ng/mL testosterone (Testo) or in vehicle (Ctrl) for 7 days. (B) Quantitative
1033 analysis of ACLY relative to α-tubulin obtained from Western blot. (C) siRNA knockdown
1034 experiments of ACLY in seminal vesicle epithelial cells. ACLY protein levels in scrambled
1035 shRNA or ACLY shRNA-transfected seminal vesicle epithelial cells cultured with or without 100
1036 ng/mL testosterone were determined by Western blot. (D) Number of cells at 7 days after
1037 incubation. (E,F) Changes in oxygen consumption of seminal vesicle epithelial cells were
1038 analyzed by a flux analyzer: (E) Oxygen consumption rate (OCR) kinetics of seminal vesicle
1039 epithelial cells transfected with scrambled shRNA or ACLY shRNA. (F) Basal OCR. (G) The
1040 impact of ACLY knockdown on testosterone-induced fatty acid synthesis was measured. These
1041 measurements were normalized based on cell count and viability. The viability of the cells before
1042 experiments was 67-81%. (H-I) Fatty acid composition in the cultured supernatants was analyzed
1043 using gas chromatography. (H) Palmitate (C16:0). (I) Stearic acid (C18:0). (J) Oleic acid (C18:1).
1044 (K-N) The effect of culture supernatants of testosterone-treated cells on sperm motility was
1045 evaluated, especially after ACLY knockdown. (K) Motile. (L) Progressive motile. (M) Straight-
1046 Line Velocity; VSL. (N) Linearity; LIN. Data are mean ± SEM. n=3-6 independent replicates.
1047 Repeated experiments were performed with cells recovered from 3 wells containing pooled cells
1048 from 3 to 5 mice. Student's t-test was used for comparison between the two groups. Percentage
1049 data were subjected to arcsine transformation before statistical analysis. (B) Significance was
1050 tested in comparison using Student’s t-test. (D,G-M) A two-way ANOVA was performed. Tukey's
1051 Honest Significant Difference test was performed as a post hoc test. (D) Both the ACLY
1052 knockdown and testosterone treatment were significant. The interaction was significant. (G) Both
1053 the ACLY knockdown and testosterone treatment were significant. The interaction was not
1054 significant. (H,I) Only the ACLY knockdown were significant. The interaction was not significant.
1055 (J) Both the ACLY knockdown and testosterone treatment were significant. The interaction was
1056 significant. (F,N) Since the results of the Bartlett test were significant, a two-way ANOVA using
1057 a generalized linear model was performed. Games-Howell was performed as a post hoc test. (E)
1058 Only the ACLY knockdown were significant. The interaction was not significant. (N)
1059 Testosterone treatment were significant. The interaction was significant. Different letters
1060 represent significantly different groups.
1061

1062 **Fig.8**

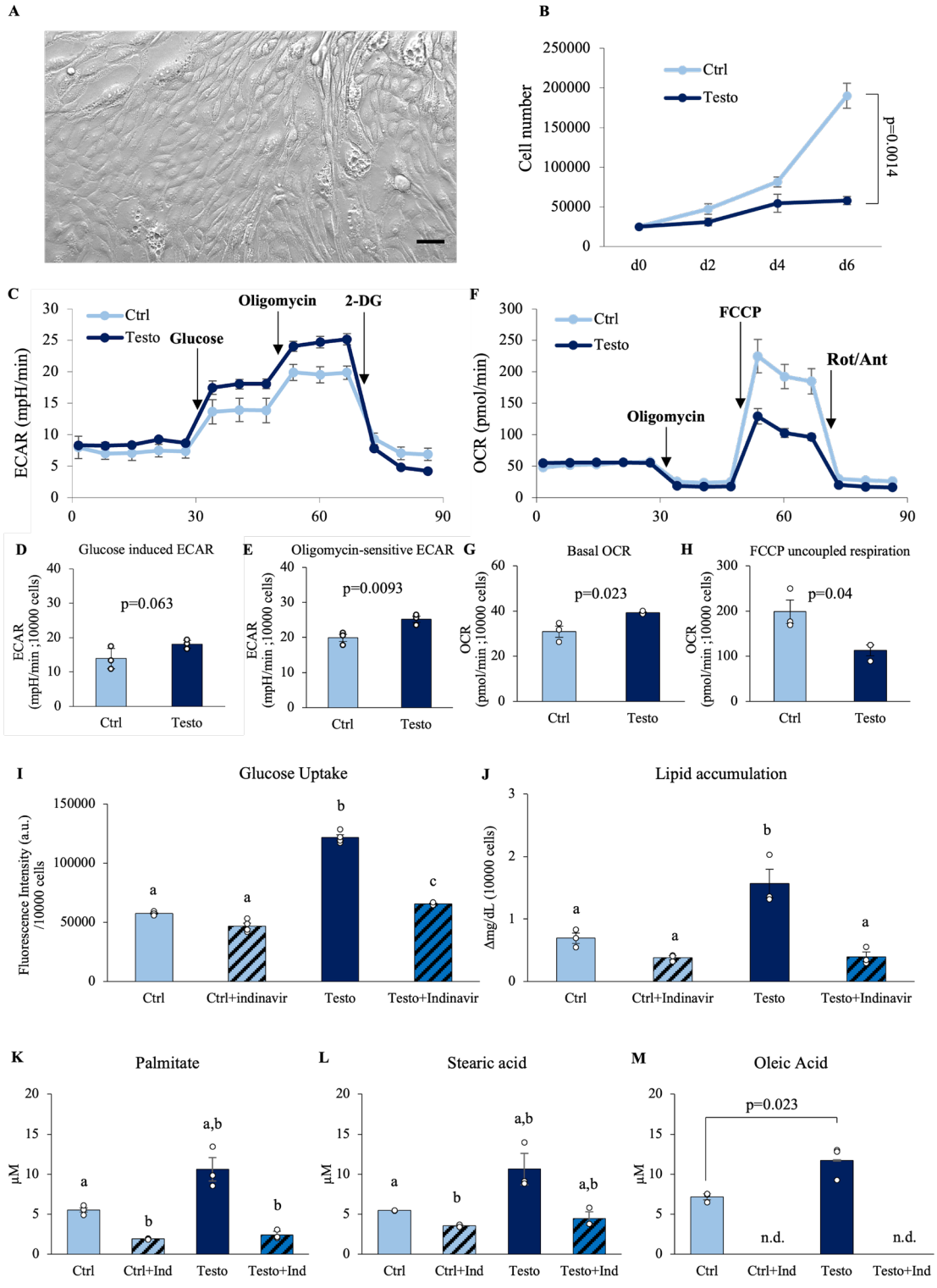

1063

1064 **Figure 8. Testosterone regulates the metabolic activity of human seminal vesicle epithelial**
1065 **cells.** (A) Representative image of human seminal vesicle epithelial cells. (B) Growth curves of

1066 seminal vesicle epithelial cells with 100 ng/mL testosterone (Testo) or without (Ctrl). (C-H)
1067 Extracellular acidification rate (ECAR) kinetics and Oxygen consumption rate (OCR) kinetics of
1068 human seminal vesicle epithelial cells after 6 days of culture with or without 100 ng/mL
1069 testosterone using a flux analyzer. (D) Glucose induced ECAR and (E) Oligomycin-sensitive
1070 ECAR. (G) Basal OCR, (H) FCCP uncoupled respiration. (I) The glucose uptake ability of
1071 seminal vesicle epithelial cells was detected using fluorescence-tagged glucose. (J) Lipid
1072 accumulation in the medium where human seminal vesicle epithelial cells were incubated for 24
1073 hours. (K-M) Fatty acid composition in the cultured supernatants was analyzed using gas
1074 chromatography. (K) Palmitate (C16:0). (L) Stearic acid (C18:0). (M) Oleic acid (C18:1). Data
1075 are mean ± SEM. n=3 independent replicates. Student's t-test was used for comparison between
1076 the two groups. (C-J) These measurements were normalized based on cell count and viability. The
1077 viability of the cells before experiments was 88-96%. (I,K,L) Since the results of the Bartlett test
1078 were significant, a two-way ANOVA using a generalized linear model was performed. Games-
1079 Howell was performed as a post hoc test. Both the Indinavir and testosterone treatment were
1080 significant. The interaction was significant. (J) A two-way ANOVA was performed. Tukey's
1081 Honest Significant Difference test was performed as a post hoc test. Both the Indinavir and
1082 testosterone treatment were significant. The interaction was significant. Different letters represent
1083 significantly different groups.
1084
1085

1086 **Fig.9**

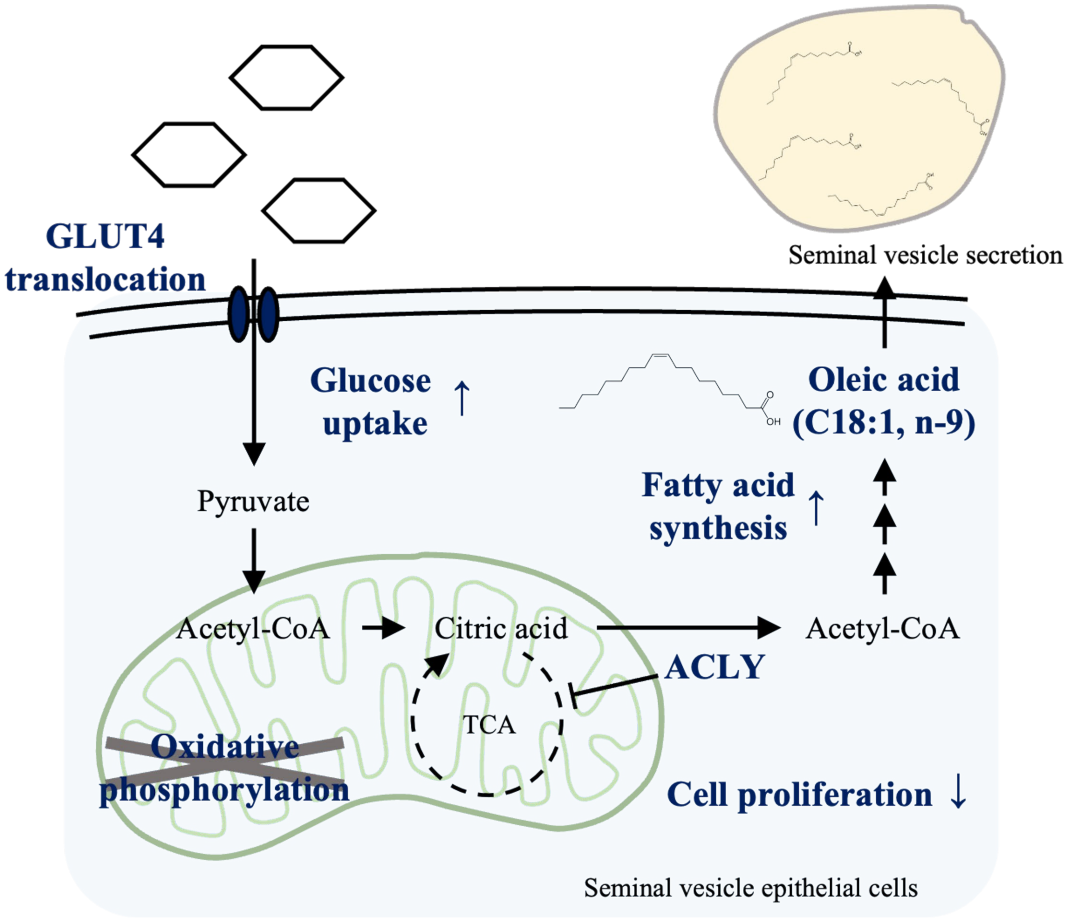

1087

1088 **Figure 9. Testosterone-induced metabolic reprogramming in seminal vesicle epithelial cells.**
1089 Testosterone promotes glucose uptake by changes in the localization of GLUT4 in seminal vesicle
1090 epithelial cells. ATP-citrate-lyase (ACLY) activated by testosterone promotes fatty acid synthesis
1091 by skipping some tricarboxylic acid (TCA) cycle steps. Simultaneously, cell proliferation in the
1092 epididymal epithelial cells is suppressed. Testosterone also promotes the synthesis of oleic acid
1093 from acetyl-CoA synthesized by ACLY.

1094

1095 **Supplemental Figure 1**

A

	Average	SEM
Motility (%)	91.5	7.5
Progressive motile (%)	57.5	6.6
VCL (μm/sec)	190.8	9.4
VSL (μm/sec)	74.7	3.5
LIN (%)	38.0	3.6
Viscosity of HTF (mPa·s)	0.8	0.01

B

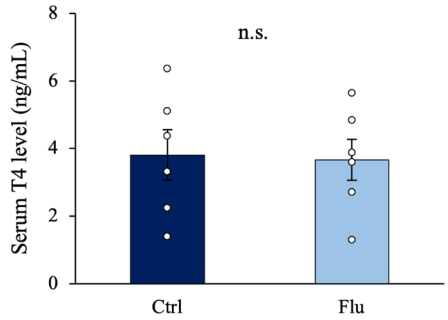

C

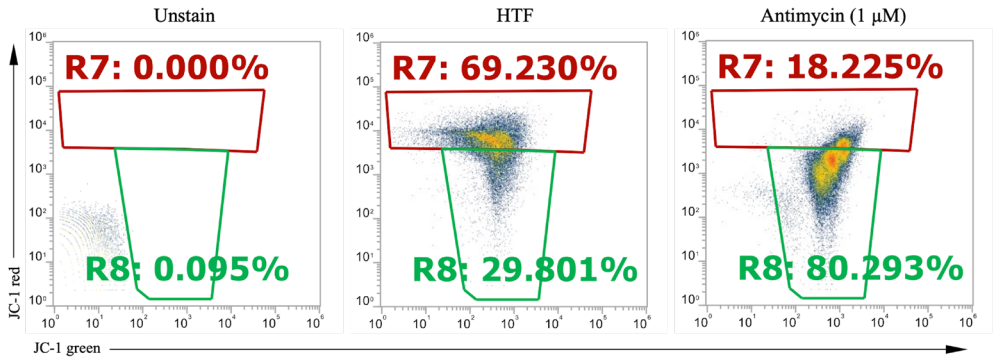

D

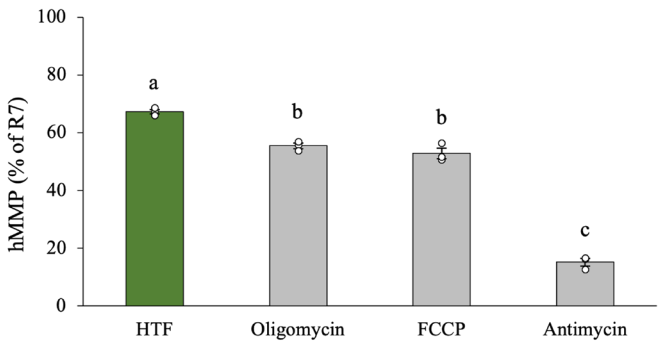

E

		No. of oocytes		
		Inseminated	Cleaved	(%)
	HTF	349	313	89.7
+SV extracts	Ctrl	86	23	26.7
+SV extracts	Flu	94	13	13.8

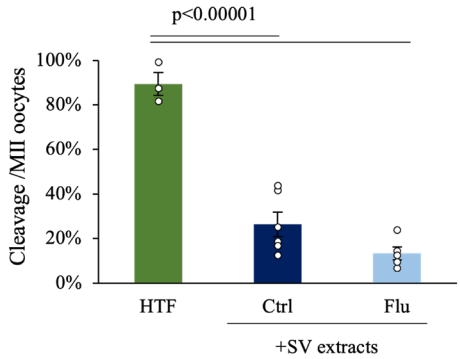

1096

1097 **Supplemental Figure 1. Sperm quality control data and exploratory research into the effects**
1098 **of seminal vesicle secretions on sperm fertilization** (A) The baseline information for the

1099 epididymal sperm used in Fig 1 and Supplemental Fig 2A. Curvi-Linear Velocity; VCL, Straight-
1100 Line Velocity; VSL and Linearity; LIN is the ratio of VSL to VCL of sperm incubated in HTF
1101 medium one hour. (B) Serum testosterone levels in seminal vesicle secretion donors. (C) Typical
1102 flow cytometry patterns for JC-1 staining From left to right: Unstained, untreated (HTF), and
1103 antimycin-treated sperm. R7 and R8 were gated to obtain positive rates of over 60% for HTF and
1104 antimycin, respectively. (D) The effect of various drugs on the proportion of high mitochondrial
1105 membrane potential (hMMP; R7). Data are mean ± SEM. At least three independent replicates.
1106 (B) Significance was tested in comparison using Student's t-test. (D) Percentage data were
1107 subjected to arcsine transformation before statistical analysis. Differences between groups were
1108 assessed by one-way analysis of variance (ANOVA). When ANOVA was significant, differences
1109 among values were analyzed by Tukey's Honest Significant Difference test for multiple
1110 comparisons. Different letters represent significantly different groups.
1111

1112 **Supplemental Figure 2**

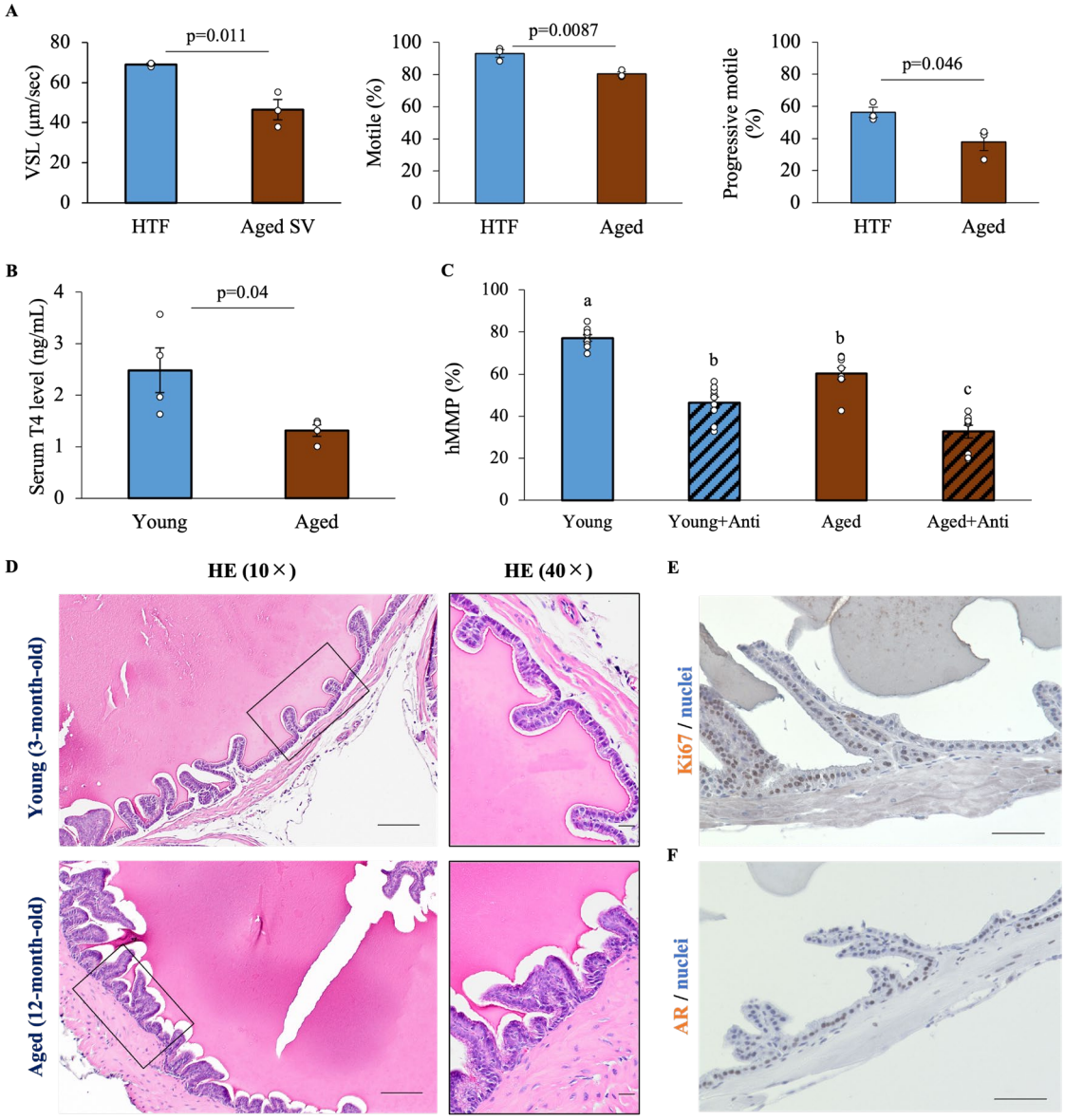

1113

1114 **Supplemental Figure 2. Characteristics of the seminal vesicle in aging mice** (A) The effects
1115 of secretions from aged seminal vesicle fluid on sperm motility. Straight-Line Velocity; VSL,
1116 Motile, and Progressive motile. (B) Serum testosterone (T4) levels in young (3 months old) or
1117 aged (12 months) mice. (C) The high mitochondrial membrane potential (hMMP) was checked
1118 by the JC-1 kit. (D) Hematoxylin/Eosin (HE) staining in seminal vesicles of young and aged
1119 mice. Scale bar=50 μm for left panel and 20 μm for right panel. (E) Representative images
1120 staining for Ki67. Scale bar=50 μm. (F) The localization of the androgen receptor (AR; NR3C4)
1121 in the seminal vesicles of aged mice. Scale bar=50 μm. (E,F) Images were obtained at 10×

magnification. Data are mean ± SEM. At least three independent replicates. Percentage data were subjected to arcsine transformation before statistical analysis. (A,B) Significance was tested in comparison using Student's t-test. (C) A two-way ANOVA was performed. Tukey's Honest Significant Difference test was performed as a post hoc test. Both the age and antimycin treatment were significant. The interaction was not significant. Different letters represent significantly different groups.

1129 **Supplemental Figure 3**

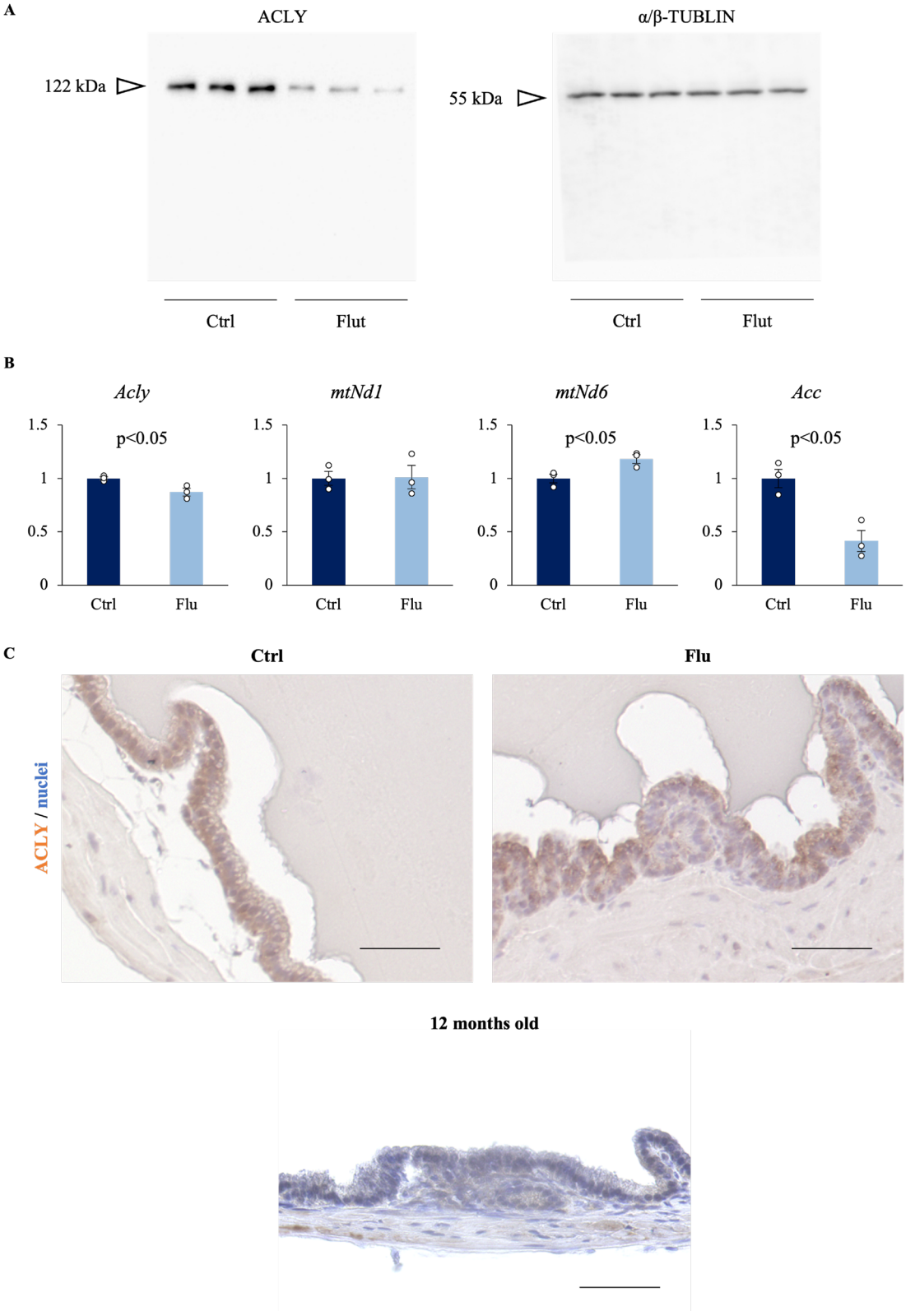

1130

1131 **Supplemental Figure 3. ACLY expression in *in vivo* seminal vesicle** (A) Representative
1132 Western blot images of ACLY and α-tubulin in three sets of seminal vesicle collected from 50
1133 mg/kg flutamide subcutaneously for 7 days (Flut) or vehicle treated mice (Ctrl). (B)
1134 Quantification of *Acly mtNd1, mtNd6 and Acc* gene expression by RT-qPCR. Data are mean ±
1135 SEM. Student's t-test was used for comparison between the two groups (n=3). (C) ACLY
1136 immunostaining: seminal vesicles from wild-type mice, flutamide-treated mice, and 12-month-
1137 old aging mice. Scale bar is 50 μm.
1138

1139 **Supplemental Figure 4**

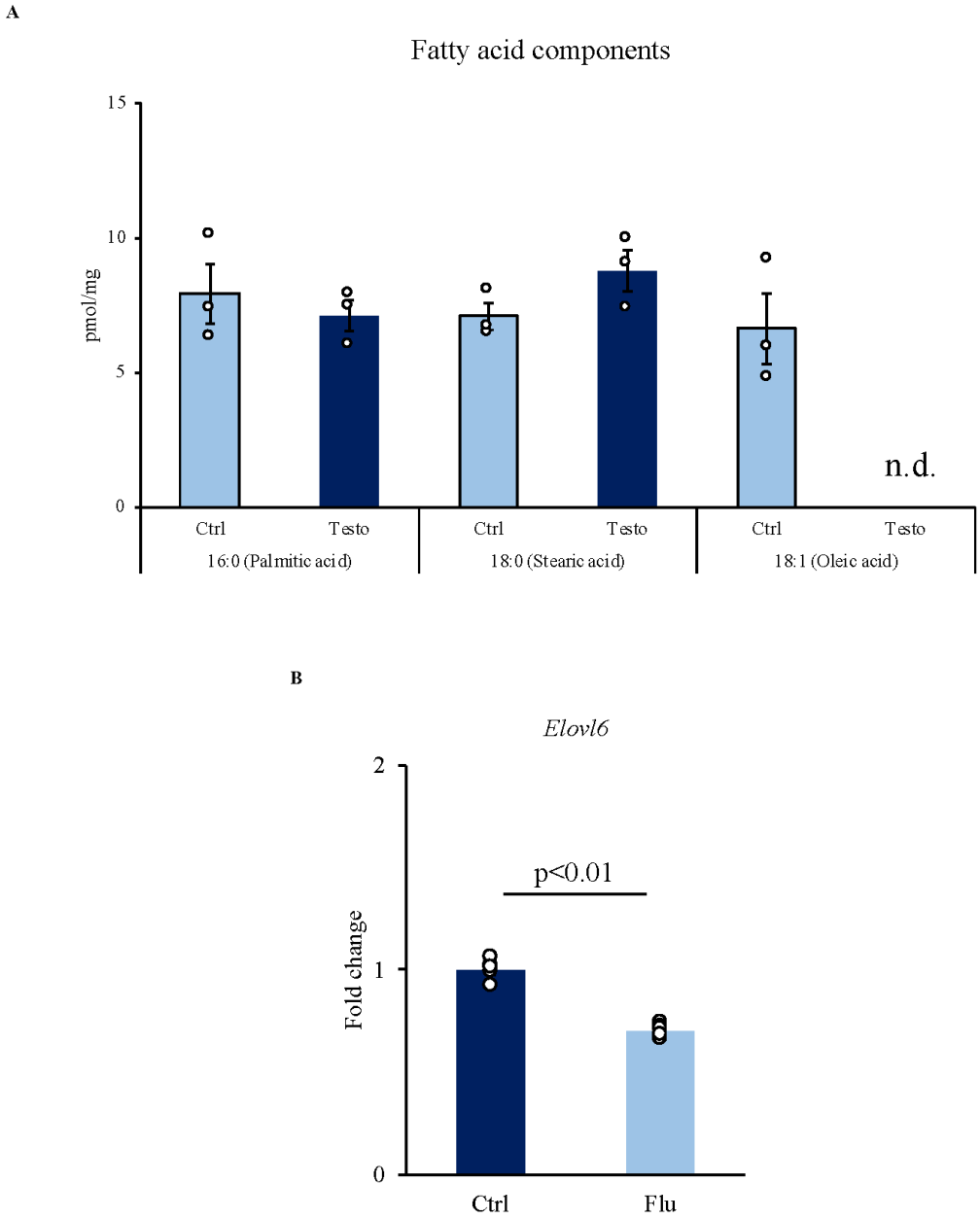

1140

1141 **Supplemental Figure 4. Oleic acid synthesis *in vivo* regulated by the testosterone-androgen**
1142 **receptor system** (A) Fatty acid composition of seminal vesicle extracts in flutamide-treated (Flu)
1143 or vehicle mice (Ctrl) pretreated with a methylation kit was analyzed by gas chromatography.
1144 *Moles contained per unit wight of seminal vesicle secretions. (B) Quantification of *Elovl6* gene
1145 expression by RT-qPCR. Data are mean ± SEM. Student's t-test was used for comparison between
1146 the two groups (n=5).

1147

1148 **Supplemental Figure 5**

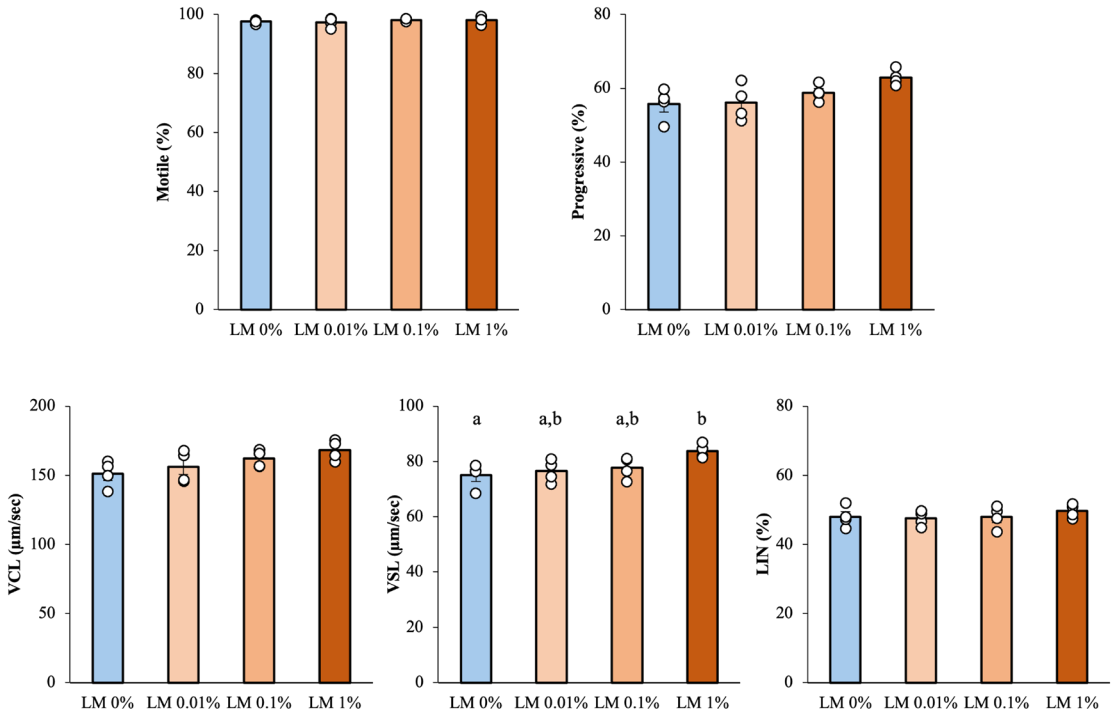

1149

1150 **Supplemental Figure 5. The effects of lipid mixture on sperm function.** The lipid mixture
1151 (LM) improves the VSL of sperm. Here, LM means that sperm were cultured in HTF medium
1152 containing a lipid mixture for 1 hour, and the control (LM 0%) means without LM. Curvi-Linear
1153 Velocity; VCL, Straight-Line Velocity; VSL and Linearity; LIN is the ratio of VSL to VCL. Data
1154 are mean ± SEM of n = 3 replicate experiments. Percentage data were subjected to arcsine
1155 transformation before statistical analysis. Differences between groups were assessed by one-way
1156 analysis of variance (ANOVA). When ANOVA was significant, differences among values were
1157 analyzed by Tukey's Honest Significant Difference test for multiple comparisons. Different letters
1158 represent significantly different groups.

1159

1160

1161 **Supplemental Figure 6**

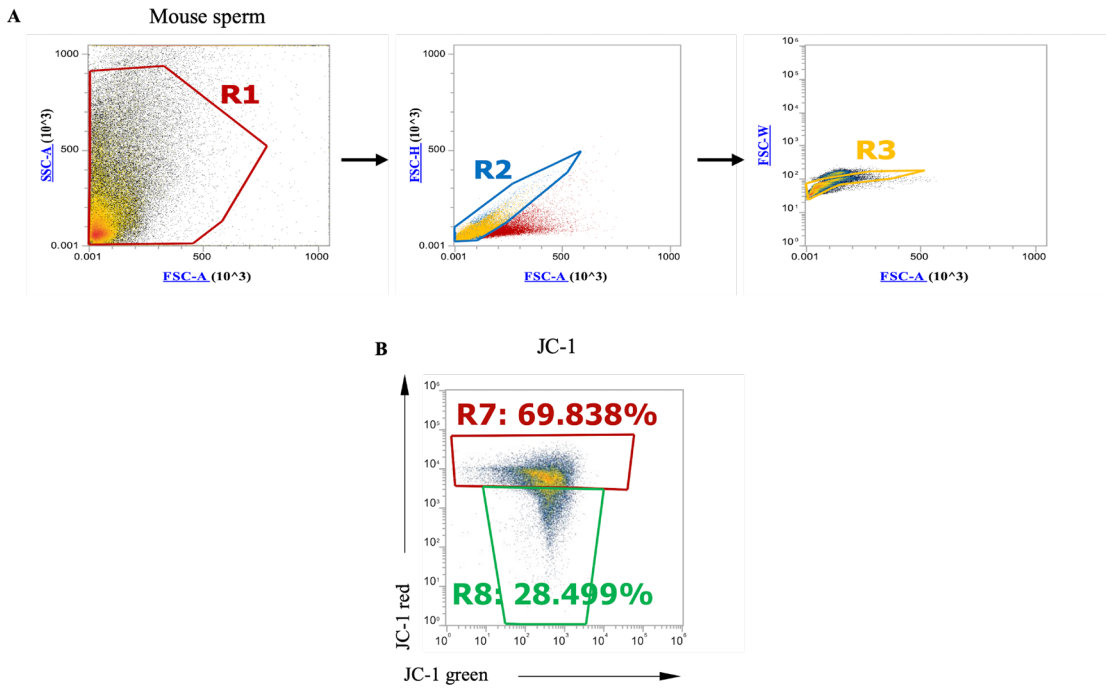

1162

1163 **Supplemental Figure 6. Gating strategy of flow cytometry for sperm** (A) Gating strategy for
1164 the selection of single sperm. Using forward scatter (FSC)-A and side scatter (SSC)-A dot plots,
1165 similar size and complexity cells were firstly selected (R1). In FSC-A and FSC-H dot plots and
1166 FSC-A and FSC-W dot plots, similar-size cells were accumulated near area; thus, using these
1167 plots, again similar-size cells were selected (R2, R3). The cells in R3 were used for below
1168 analysis. (B) The dot plots of 5,5’,6,6’-tetrachloro-1,1’,3,3’-tetraethylbenzimidazolyl
1169 carbocyanine iodide (JC-1) green (x-axis) and red (y-axis). The percentage of JC-1 red-
1170 positive sperm (R7) was used for the analysis.

1171

1172 **Supplemental Figure 7**

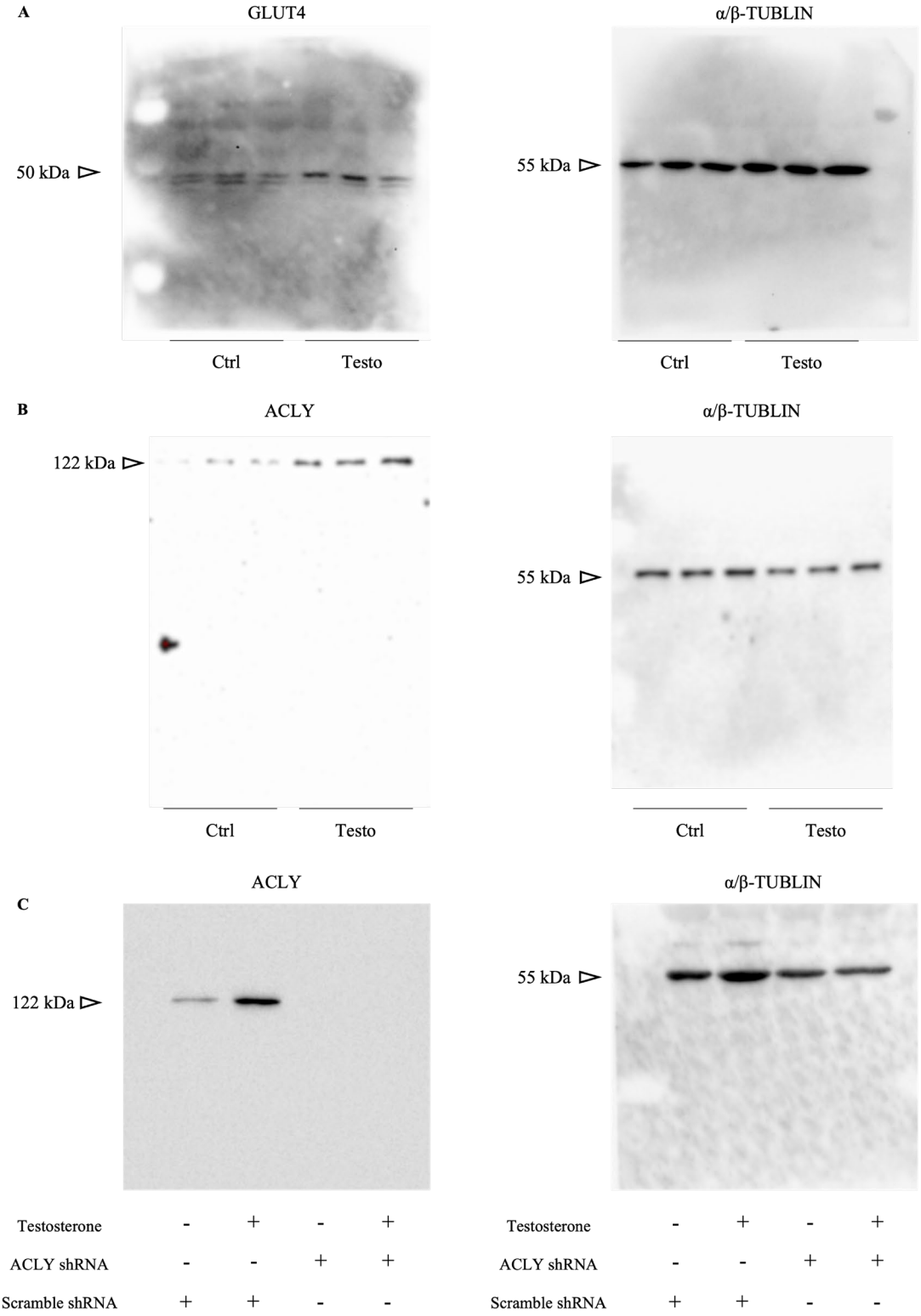

1173

1174 **Supplemental Figure 7. Full-length blotting images of western blotting** (A) Full-length

1175 blotting images of GLUT4 and α/β-TUBLIN in seminal vesicle epithelial cells cultured with

1176 100 ng/mL testosterone (Testo) or in vehicle (Ctrl) in Figure 6D. (B) Full-length blotting images
1177 of ACLY and α/β-TUBLIN in seminal vesicle epithelial cells cultured with 100 ng/mL
1178 testosterone (Testo) or in vehicle (Ctrl) in Figure 8A. (C) Full-length blotting images of ACLY
1179 and α/β-TUBLIN in seminal vesicle epithelial cells in Figure 8C. ACLY protein levels in
1180 scrambled shRNA or ACLY shRNA-transfected seminal vesicle epithelial cells cultured with or
1181 without 100 ng/mL testosterone were determined by Western blot.
1182

1183 **Supplemental Figure 8**

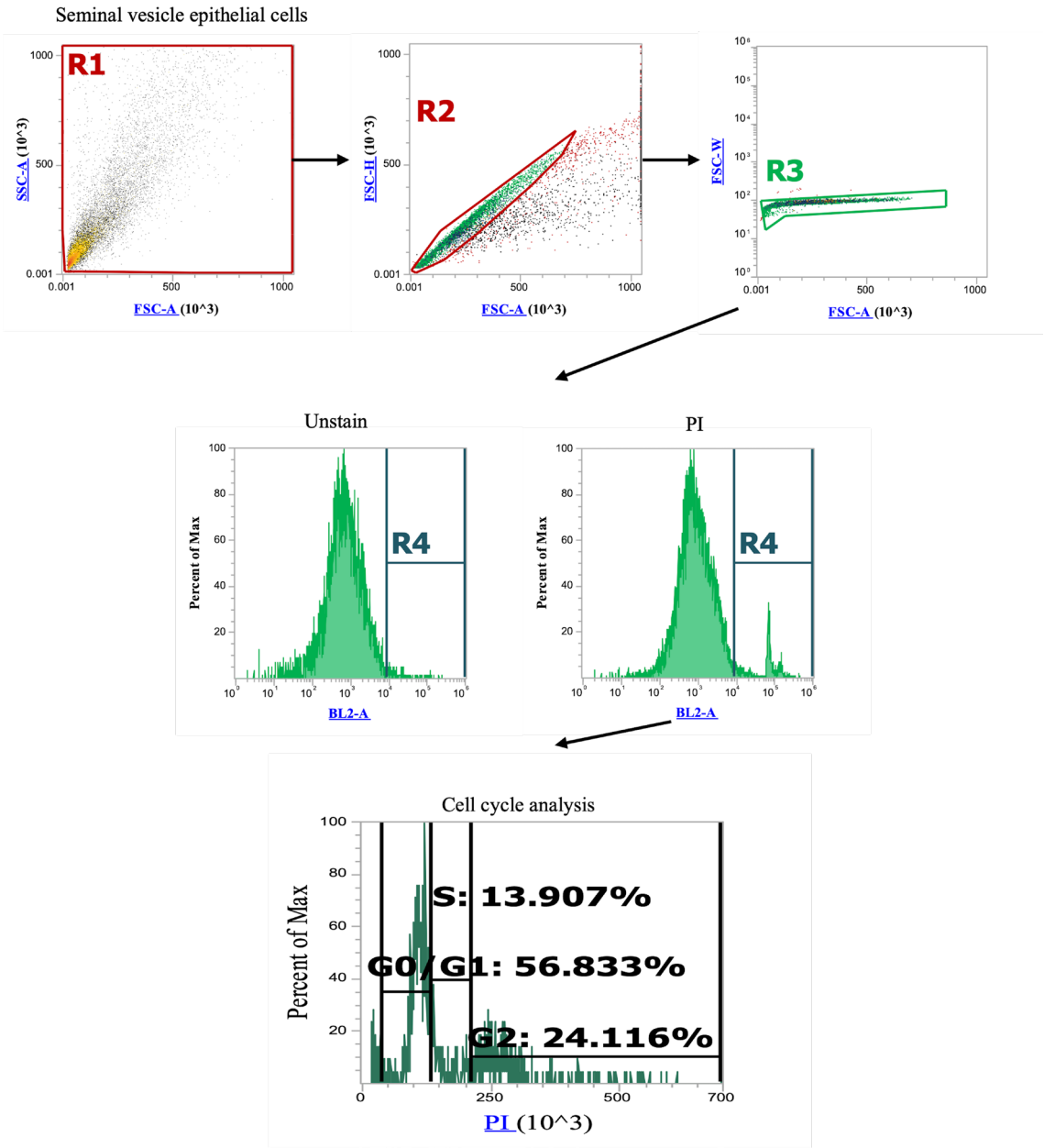

1184

1185 **Supplemental Figure 8. Gating strategy of flow cytometry for seminal vesicle epithelial cells**
1186 Gating strategy for the selection of single sperm. Using forward scatter (FSC)-A and side scatter
1187 (SSC)-A dot plots, similar size and complexity cells were firstly selected (R1). In FSC-A and
1188 FSC-H dot plots and FSC-A and FSC-W dot plots, similar-size cells were accumulated near area;
1189 thus, using these plots, again similar-size cells were selected (R2, R3). The cells in R3 were
1190 applied to the propidium iodide (PI) histogram plot. Labelling DNA with PI allows fluorescence-
1191 based analysis of the cell cycle. The intensity of PI fluorescence correlates with the amount of

1192 DNA in each cell. Comparing the G1 and G2 phases, the amount of DNA doubles in the G2 phase,
1193 so the fluorescence intensity of the cell population also doubles.
1194
1195

Table S1. Primer sequences used for quantitative real-time PCR.

Gene	Forward primer (5'→3')	Reverse primer (5'→3')
Acc	GCCTCTTCCTGACAAACGAG	TGACTGCCGAAACATCTCTG
Acly	AGGTCTCTCTGCAGCCATGT	AAGCTTTCCTCGACGTTTGA
Aco2	CTAGCCTCAGCCCAGTGAAC	CCTTCAGCCACCAGTGAAAT
Cs	CAGATGCCCACAGAGGAACA	AGCTTGGCAATGAGGTCCAT
ElovI6	CCCGAACTAGGTGACACGAT	CCGCAAGGCGTAGTAAGAGT
Fasn	AGCACACATCCTAGGCATCC	TGTCGTGTCAGTAGCCGAGT
Fh	AGCAATGCATATTGCTGCTG	CGCATACTGGACTTGCTGAA
Glut1	AAACATGGAACCACCGCTAC	AGGCCAACAGGTTCATCATC
Glut2	GCCTGTGTATGCAACCATTG	TGGCCCAATCTCAAAGAAAC
Glut3	TGTCACAGGAGAAGCAGGTG	GCTCCAATCGTGGCATAGAT
Glut4	ACTCTTGCCACACAGGCTCT	AATGGAGACTGATGCGCTCT
Hk1	TATCGGTCCAGCACGTATGC	ACATCGTGACCCACACAGTC
Hk2	GGGTAGCCACGGAGTACAAA	TGGATTGAAAGCCAACTTCC
Hmgcr	TGGAGATCATGTGCTGCTTC	GCGACTATGAGCGTGAACAA
Idh2	CCGTCTTCAGAGAGCCAATC	GAAATGGACTCGTCGGTGTT
Mdh2	GCTTTGTCTTCTCCCTCGTG	CAAAGTCCTCGCCTTTCTTG
Nd1	CAGGATGAGCCTCAAACTCC	CCGGTTTGTTTCTGCTAGGG
Nd6	GGTTGGTTGTCTTGGGTTAGC	TAGATCCCCAAGTCTCTGGA
Ogdh	ACATGGCACAGTGCATCATT	ACATCTGCAGAAACCGCTCT
Pdha	GGGGACGTCTGTTGAGAGAG	TGTGTCCATGGTAGCGGTAA
Sdhb	ACTGGTGGAACGGAGACAAG	GTTAAGCCAATGCTCGCTTC
Suclg2	CTTTGGTGGGATCGTCAACT	AACAGCTTTCTTGGCTGCAT
L19	GGCATAGGGAAGAGGAAGG	GGATGTGCTCCATGAGGATGC

1196